Supplementary Material

Conformational control of bis-urea self-assembled supramolecular pH switchable low-molecular-weight hydrogelators

Adam D. O'Donnell,[a] Alexander G. Gavriel,[a] William Christie,[a] Ann M. Chippindale,[a] Ian M. German,[b] and Wayne Hayes[a*]

[a]Department of Chemistry, University of Reading, Whiteknights, Reading, RG6 6DX, U.K.
[b]Kinectrics Inc., 17-18 Frederick Sanger Road, The Surrey Research Park, Guildford, Surrey, GU2 7YD, U.K.
Email: w.c.hayes@reading.ac.uk

Table of Contents

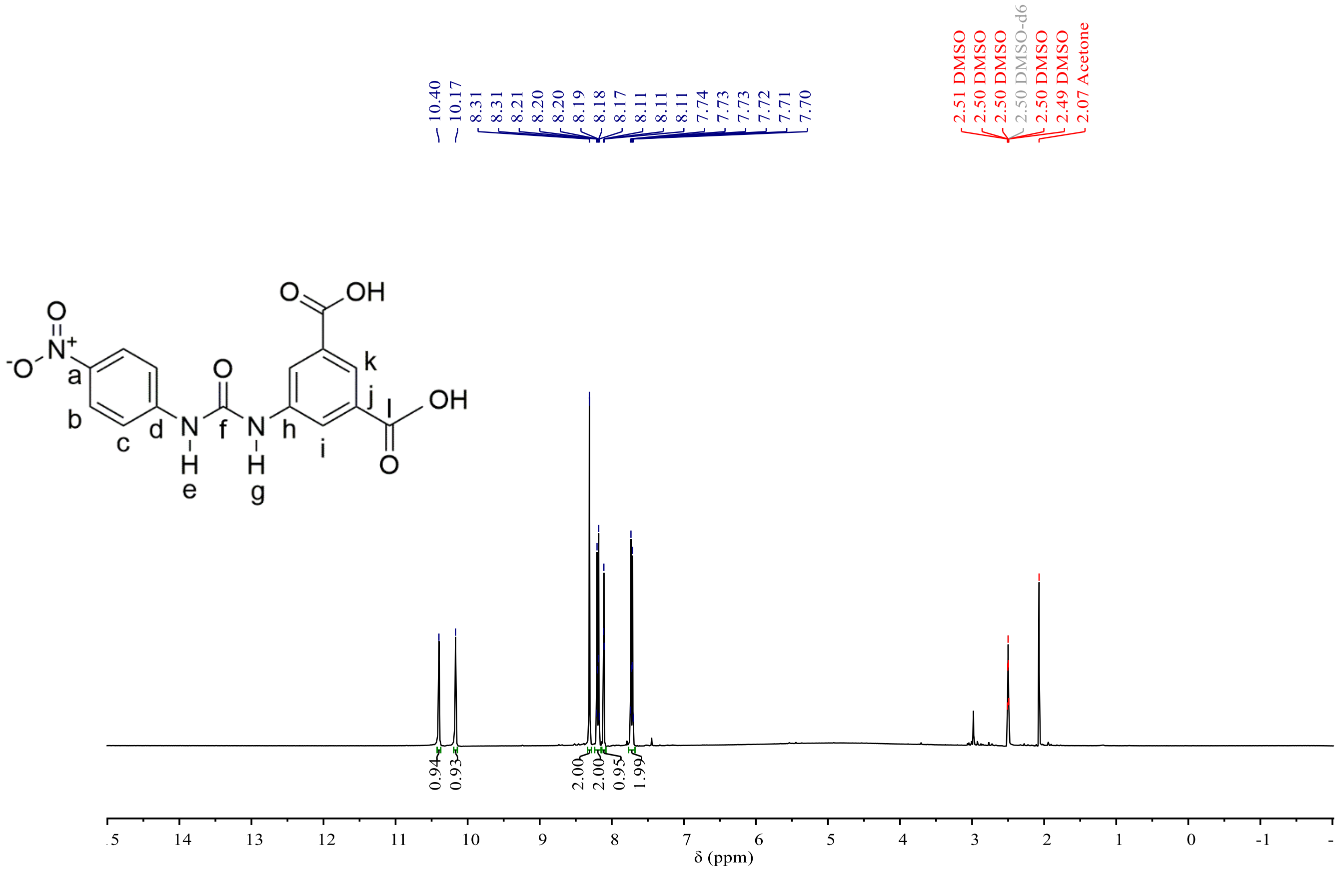

Figure S 1. ^{1}H NMR (400 MHz, DMSO-d_6, 298 K of compound **1**).

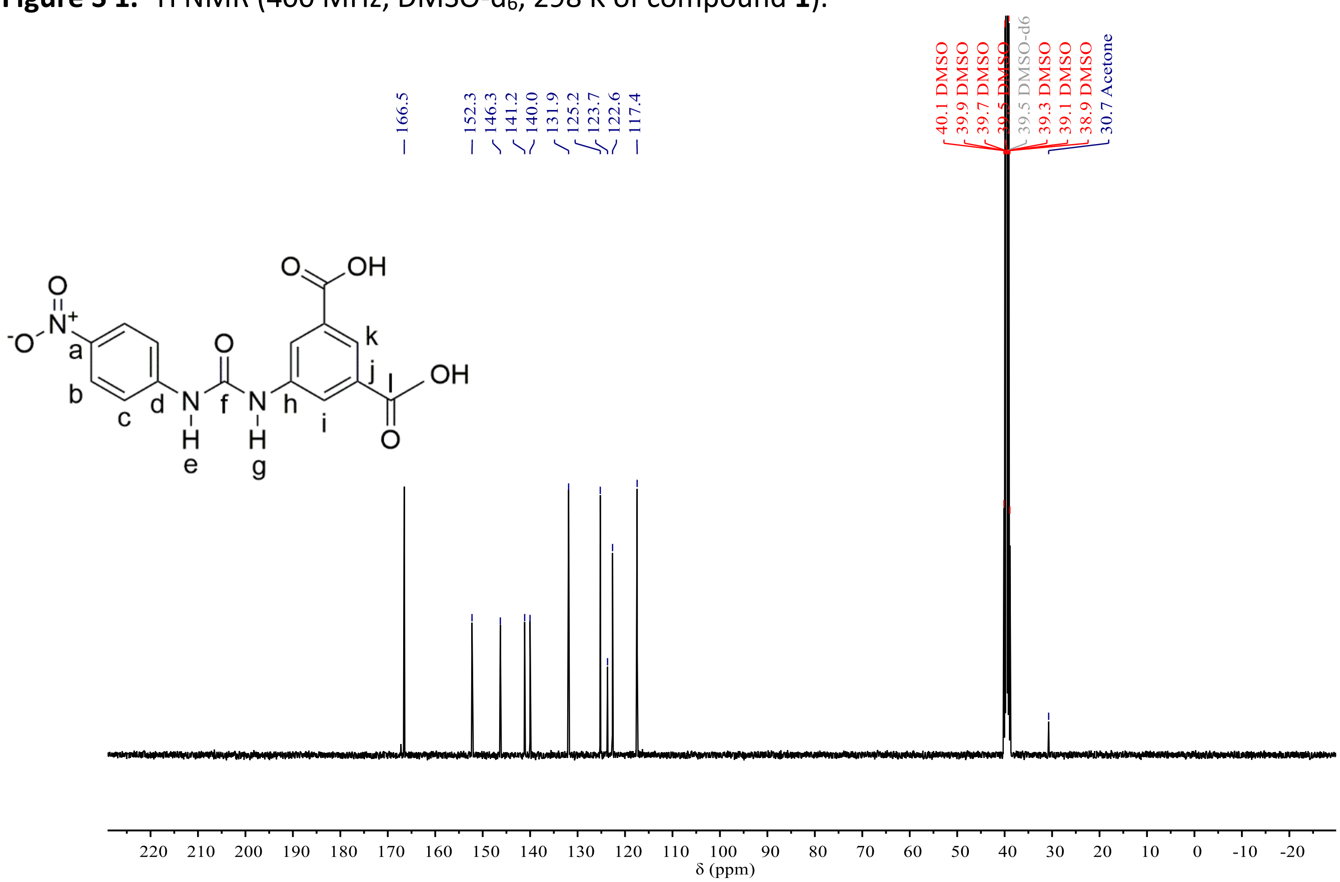

Figure S 2. $^{13}C\{H\}$ (100 MHz, DMSO-d_6, 298 K of compound **1**).

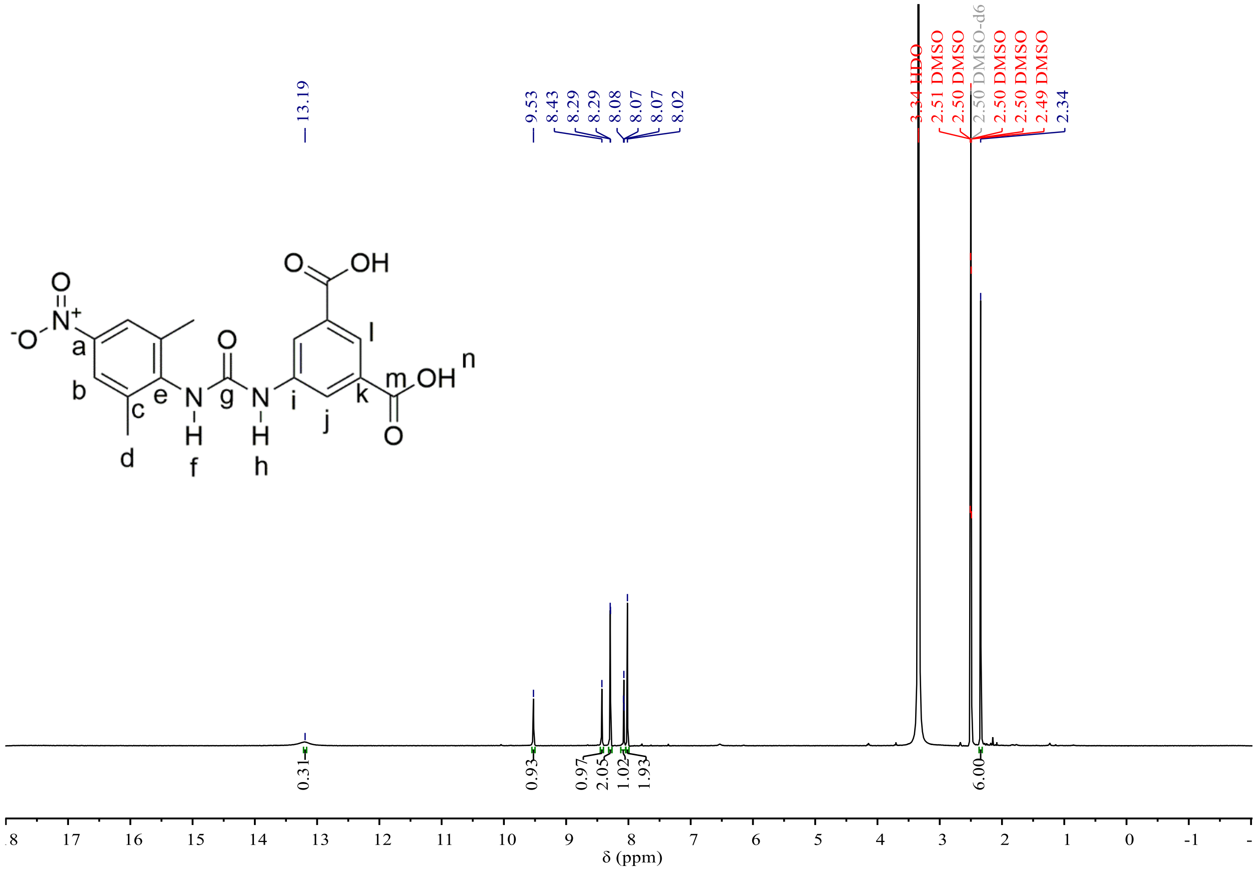

Figure S 3. ^{1}H NMR (400 MHz, DMSO-d_6, 298 K of compound **2**).

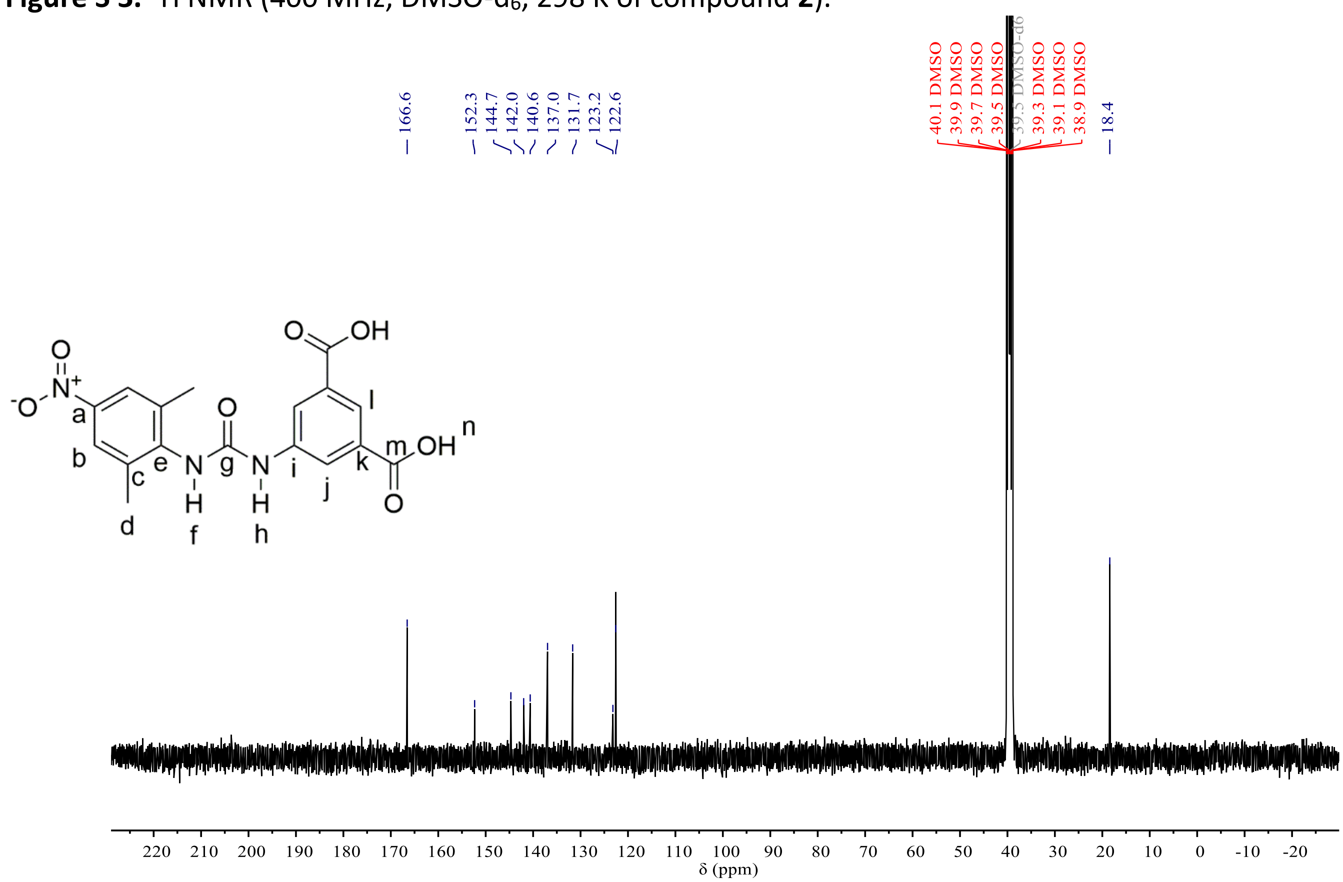

Figure S 4. ^{13}C{H} (100 MHz, DMSO-d_6, 298 K of compound **2**).

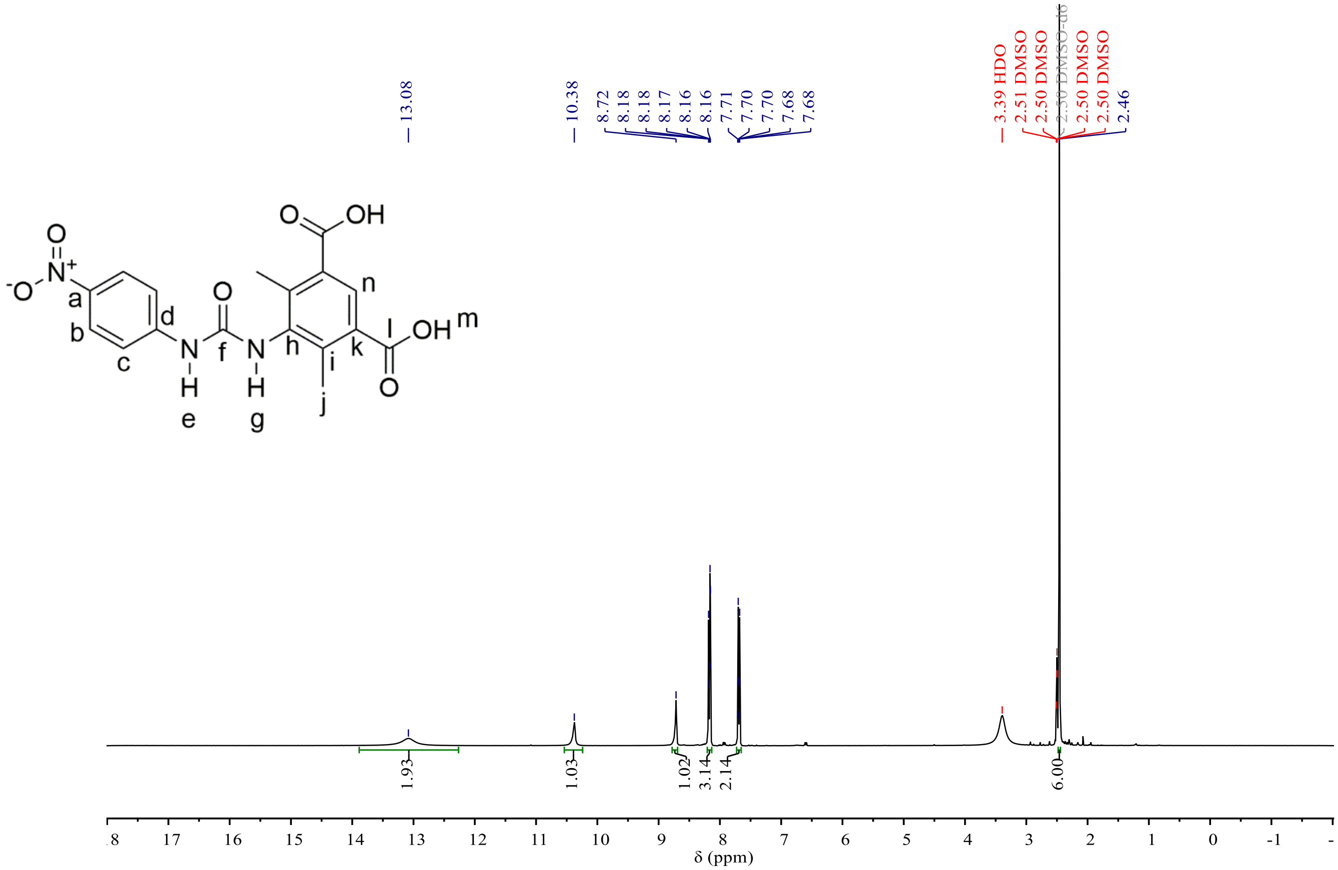

Figure S 5. ^{1}H NMR (400 MHz, DMSO-d_6, 298 K of compound **3**).

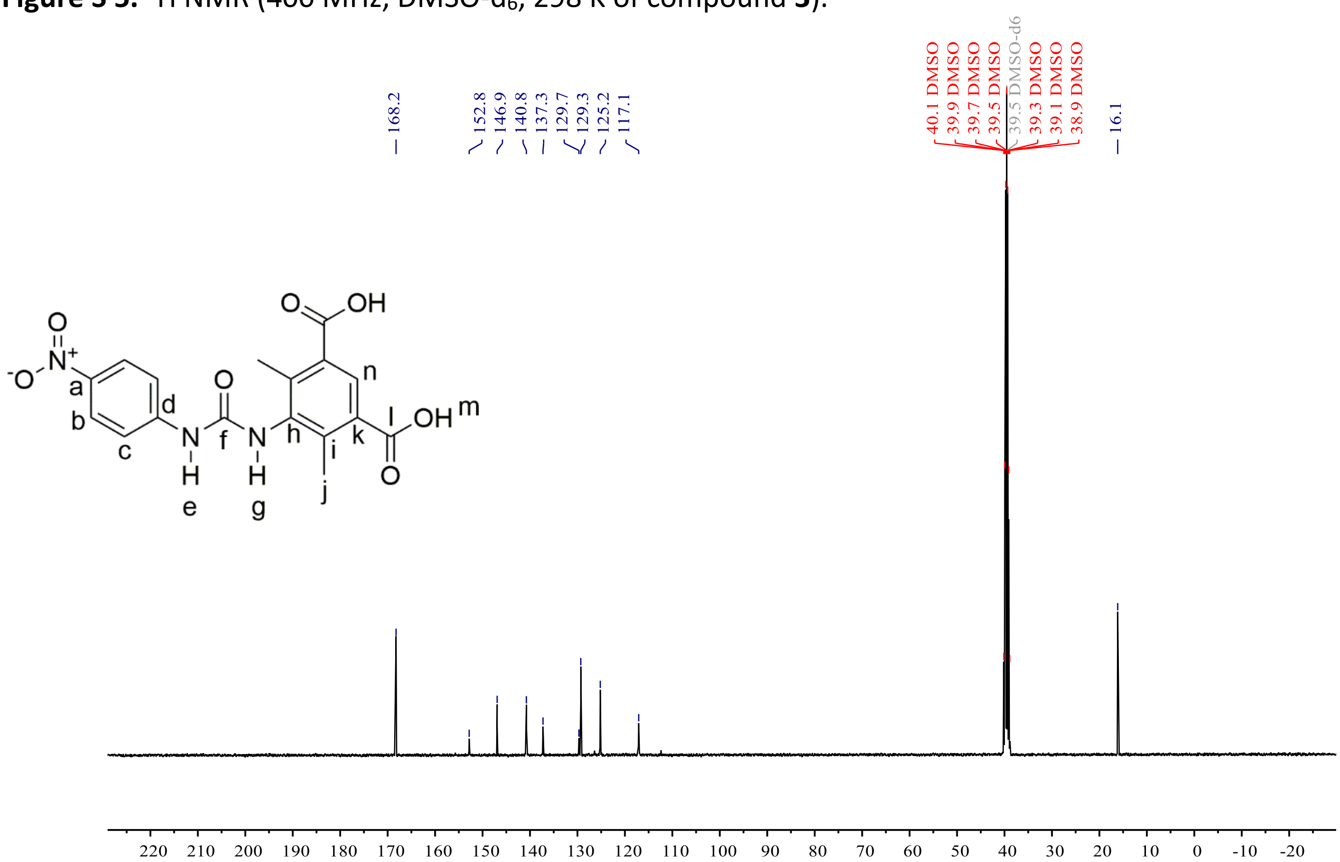

Figure S 6. $^{13}C\{H\}$ (100 MHz, DMSO-d_6, 298 K of compound **3**).

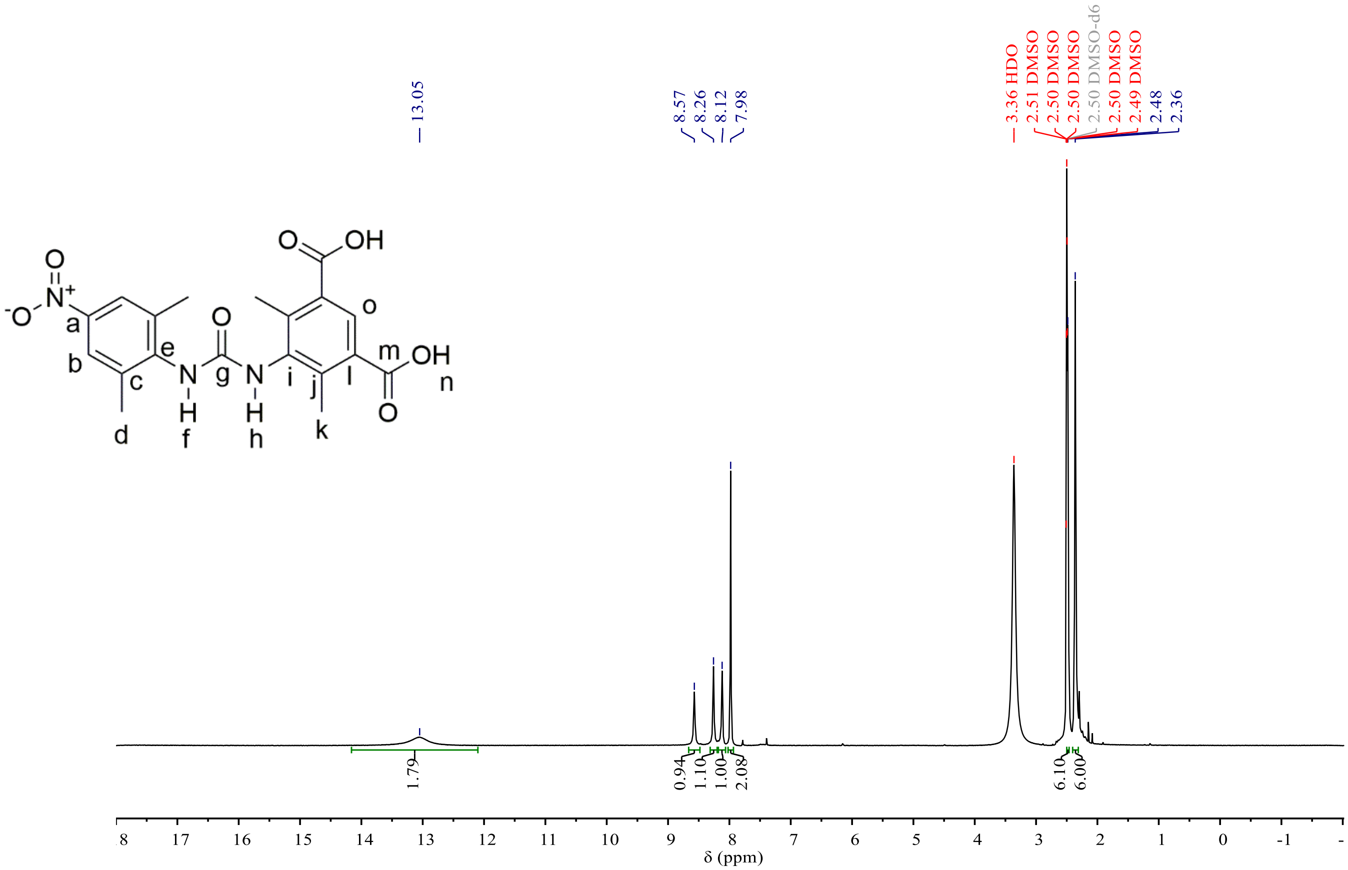

Figure S 7. ^{1}H NMR (400 MHz, DMSO-d_6, 298 K of compound **4**).

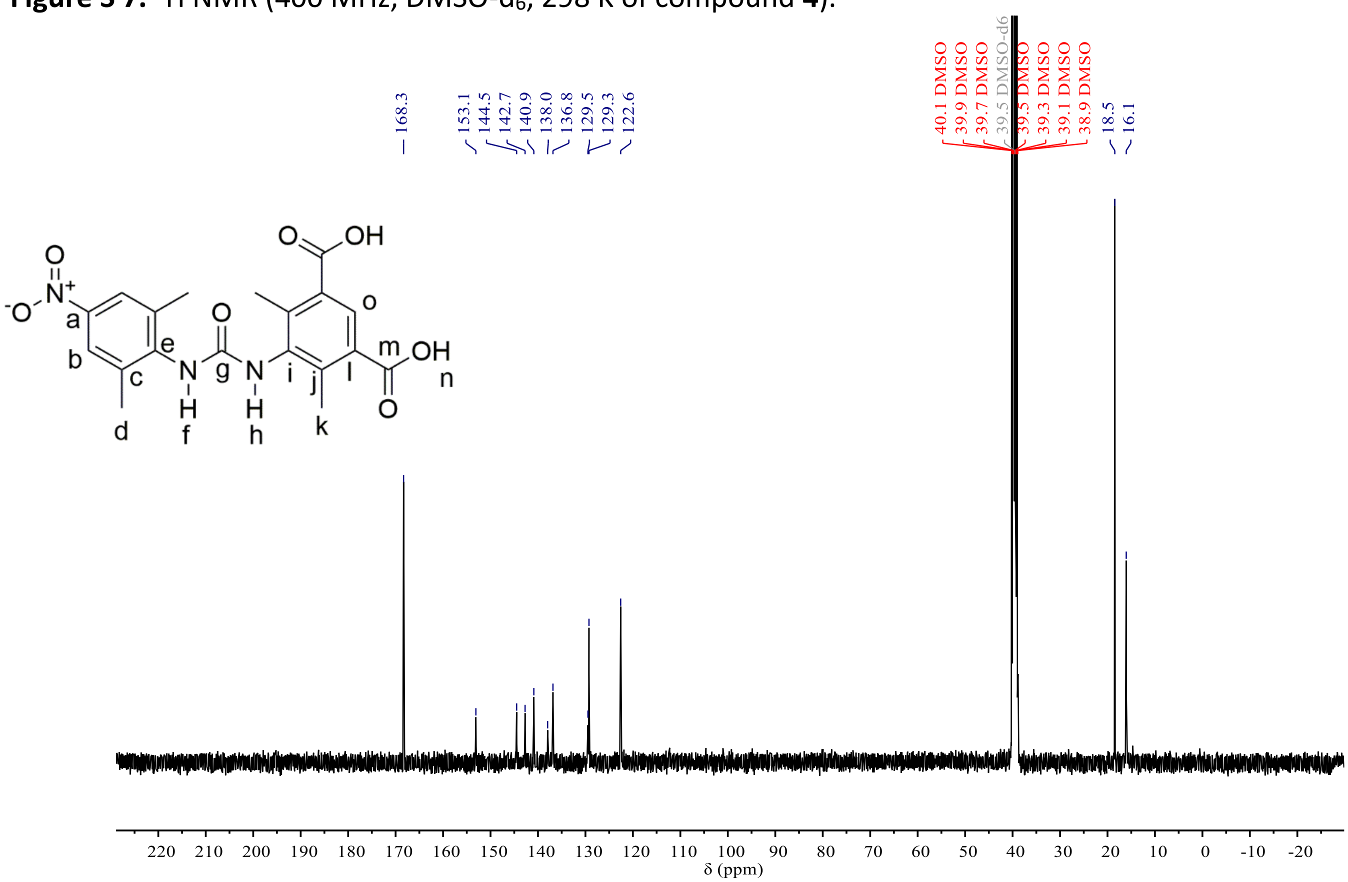

Figure S 8. $^{13}C\{H\}$ (100 MHz, DMSO-d_6, 298 K of compound **4**).

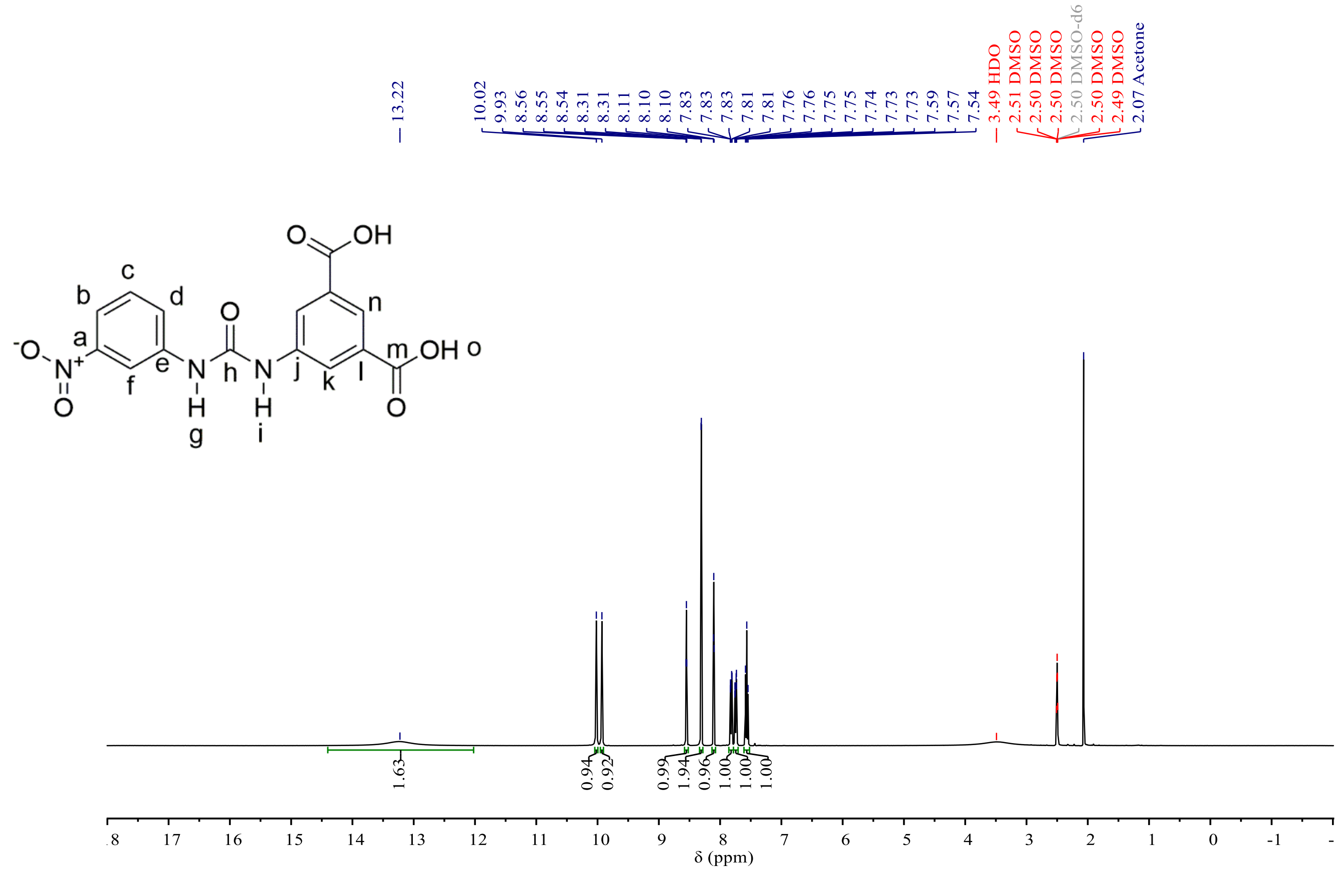

Figure S 9. ^{1}H NMR (400 MHz, DMSO-d_6, 298 K of compound **5**).

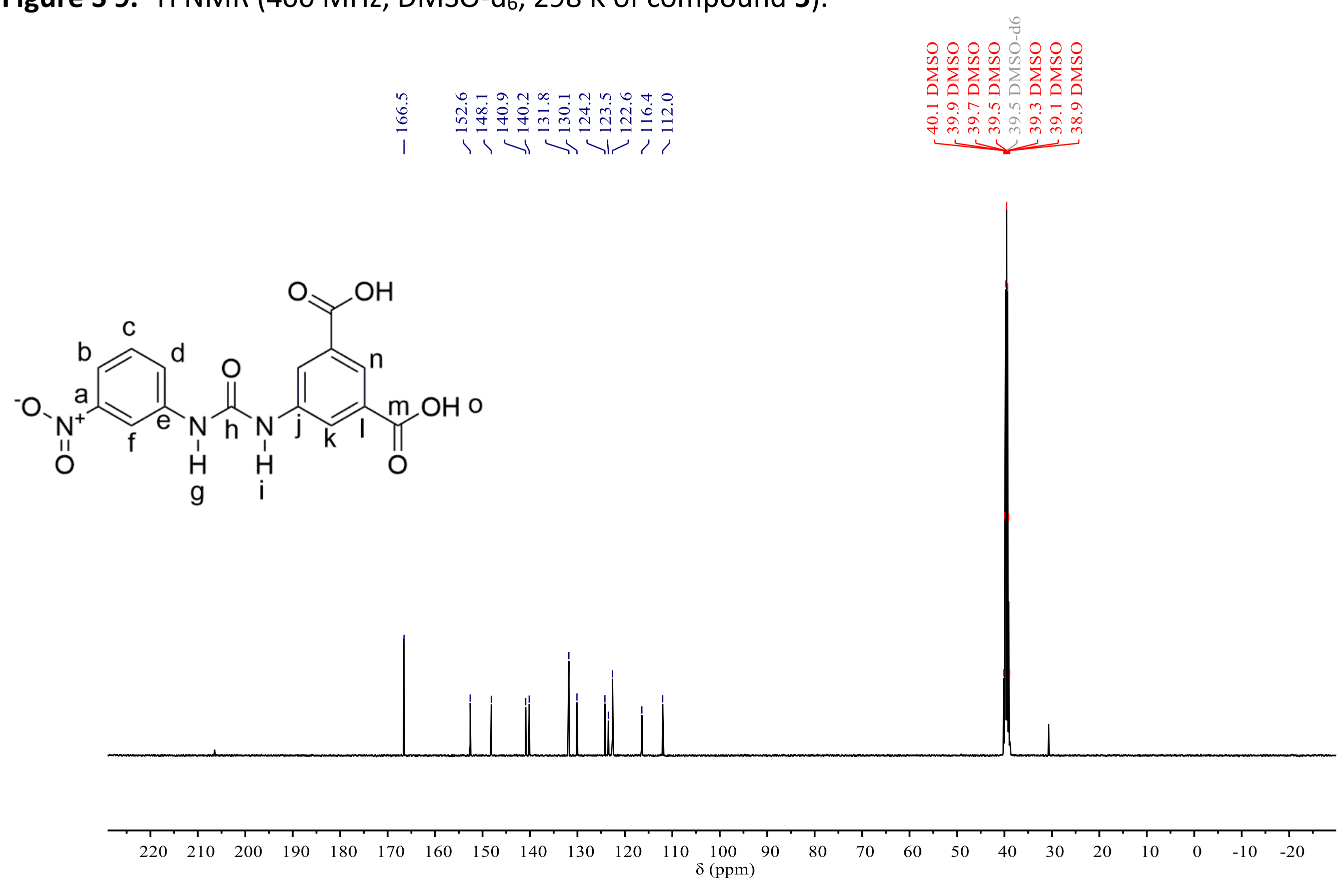

Figure S 10. $^{13}C\{H\}$ (100 MHz, DMSO-d_6, 298 K of compound **5**).

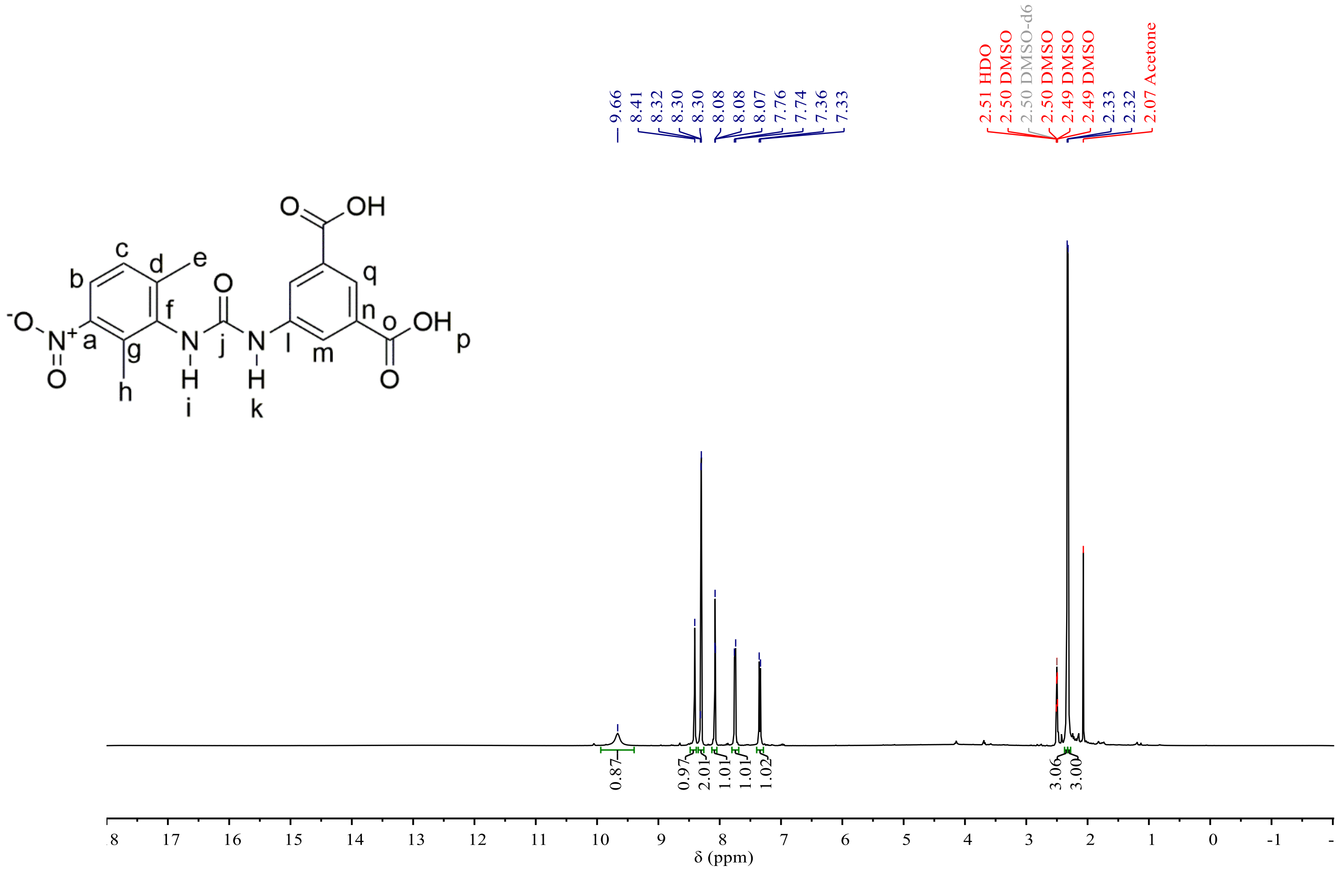

Figure S 11. ^{1}H NMR (400 MHz, DMSO-d_6, 298 K of compound **6**).

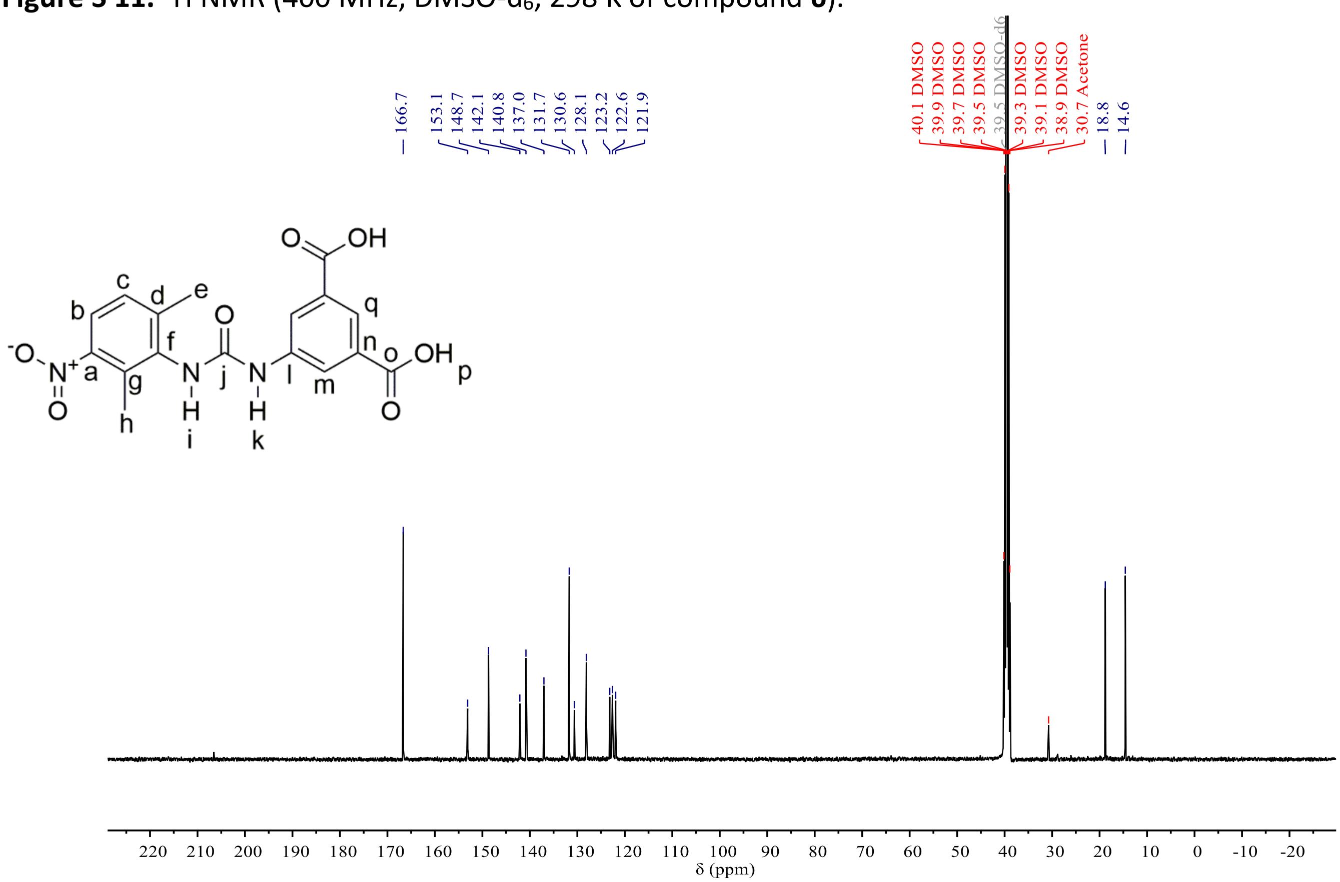

Figure S 12. ^{13}C{H} (100 MHz, DMSO-d_6, 298 K of compound **6**).

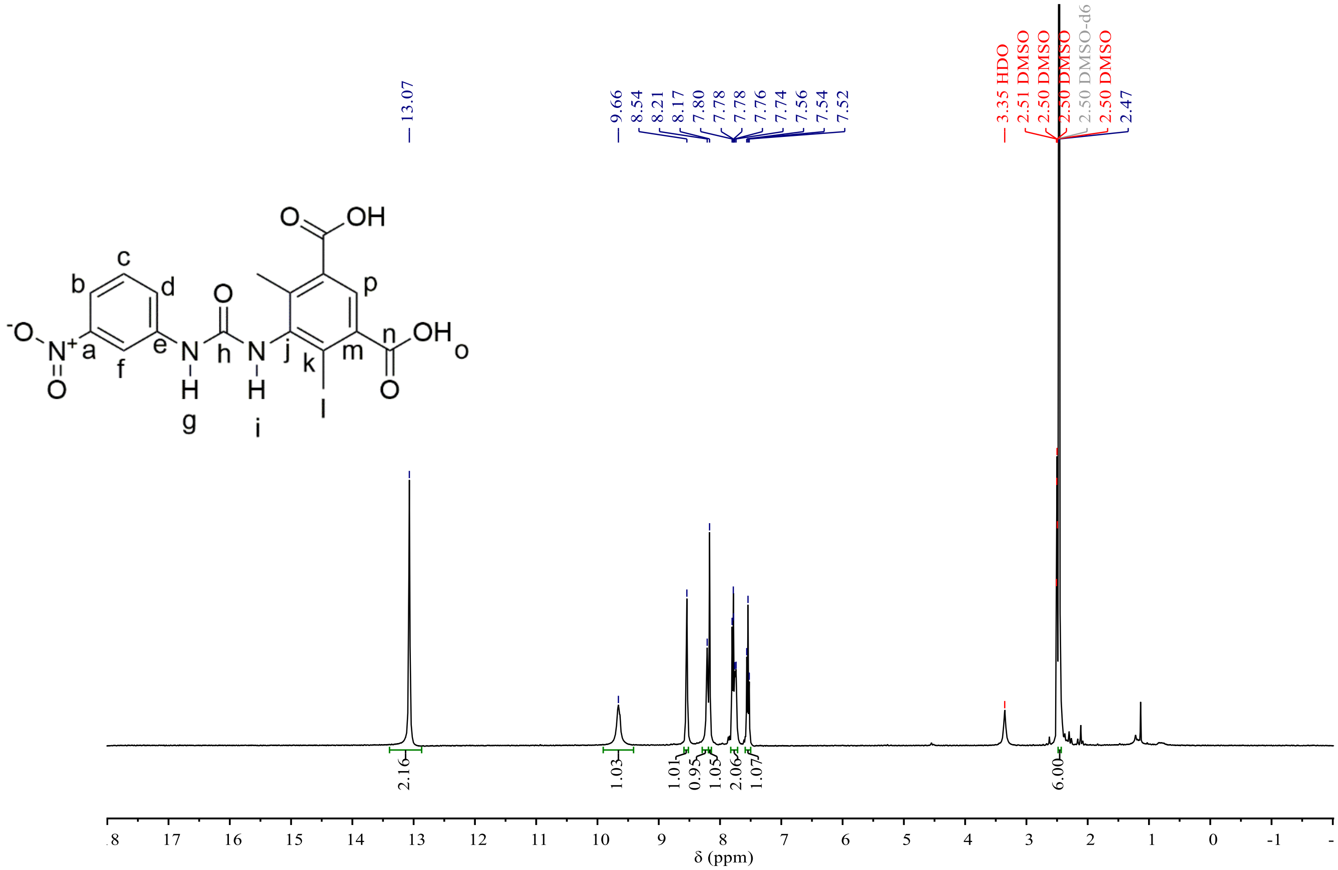

Figure S 13. ^{1}H NMR (400 MHz, DMSO-d_6, 298 K of compound **7**).

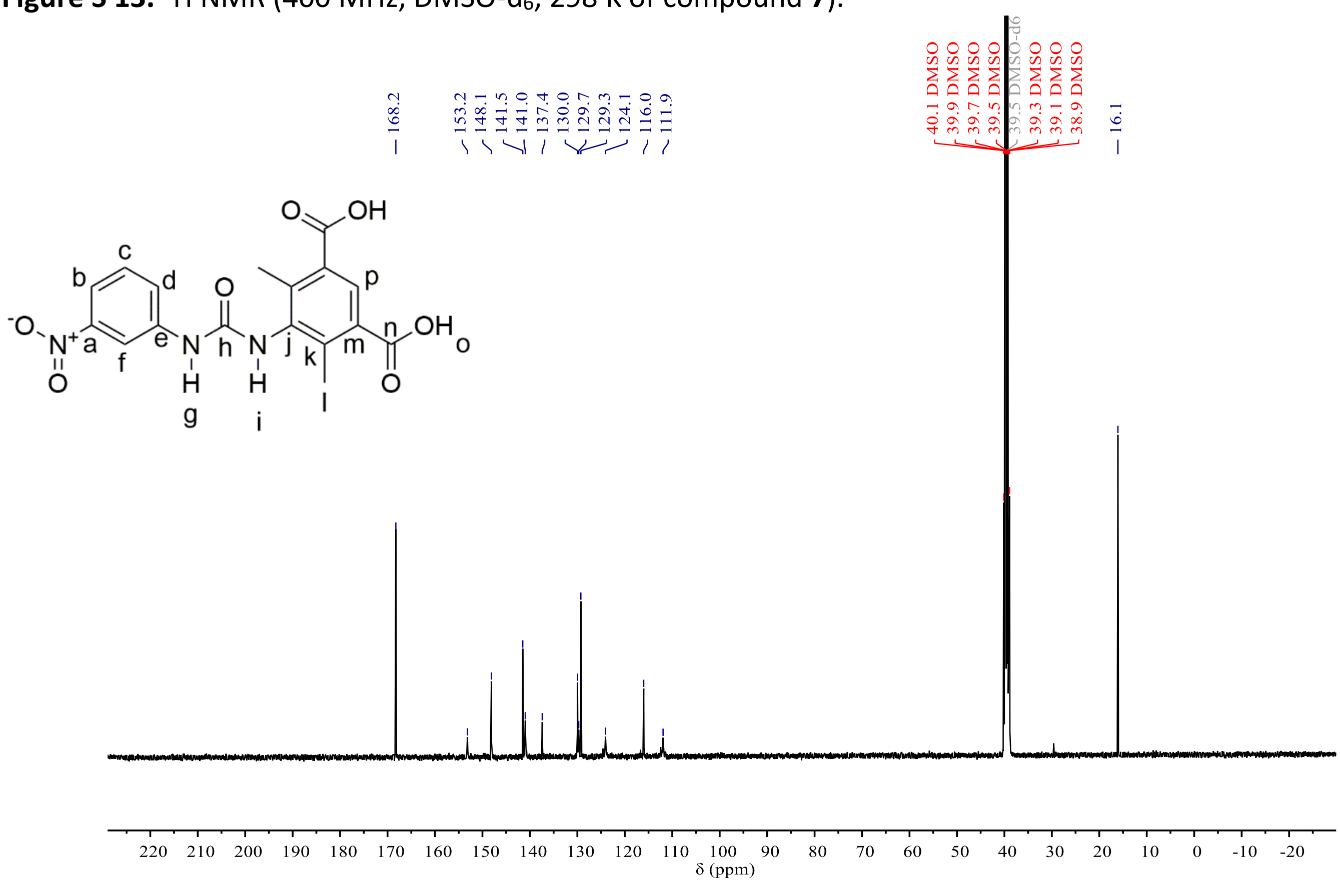

Figure S 14. $^{13}C\{H\}$ (100 MHz, DMSO-d_6, 298 K of compound **7**).

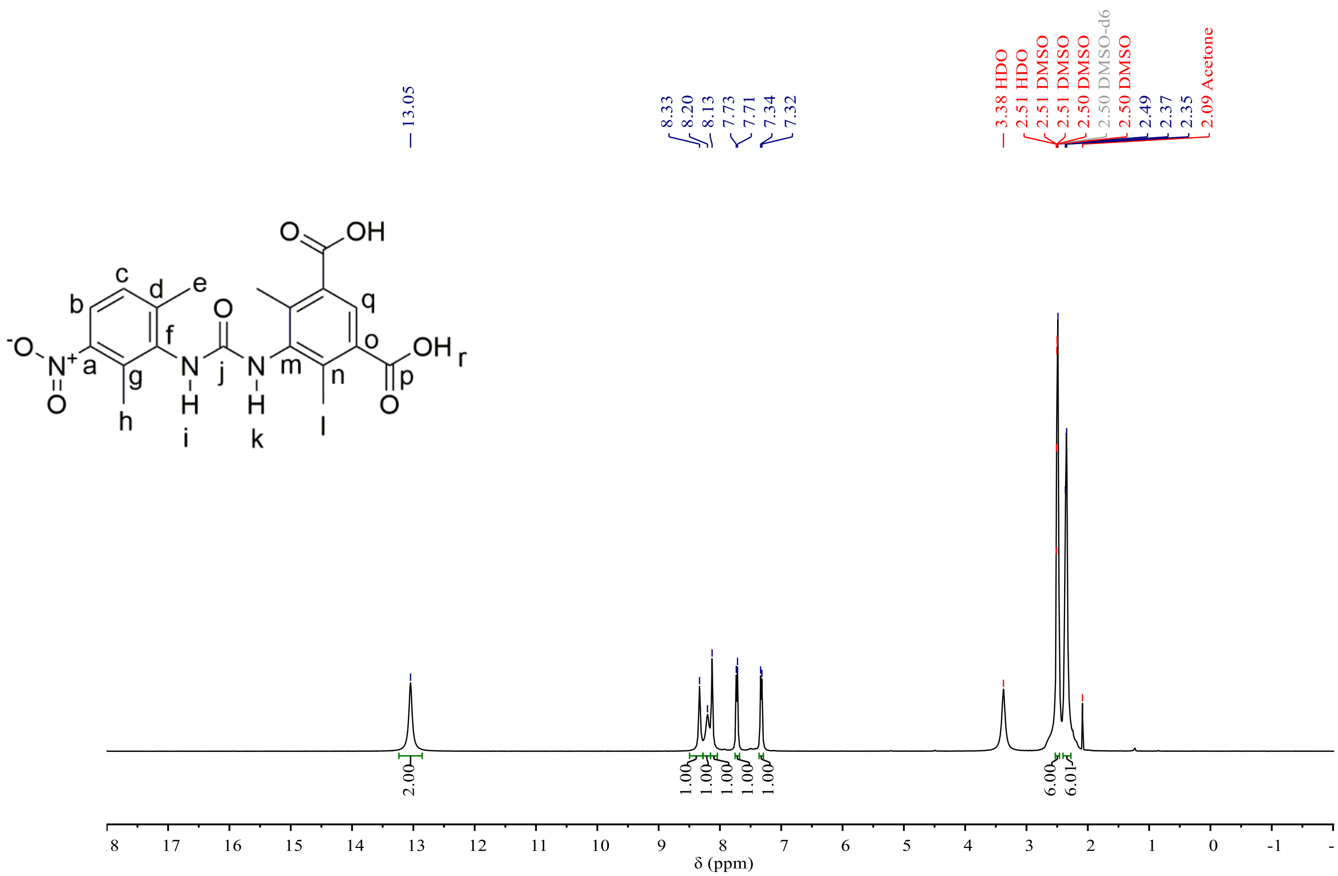

Figure S 15. ^{1}H NMR (400 MHz, DMSO-d$_6$, 298 K of compound **8**).

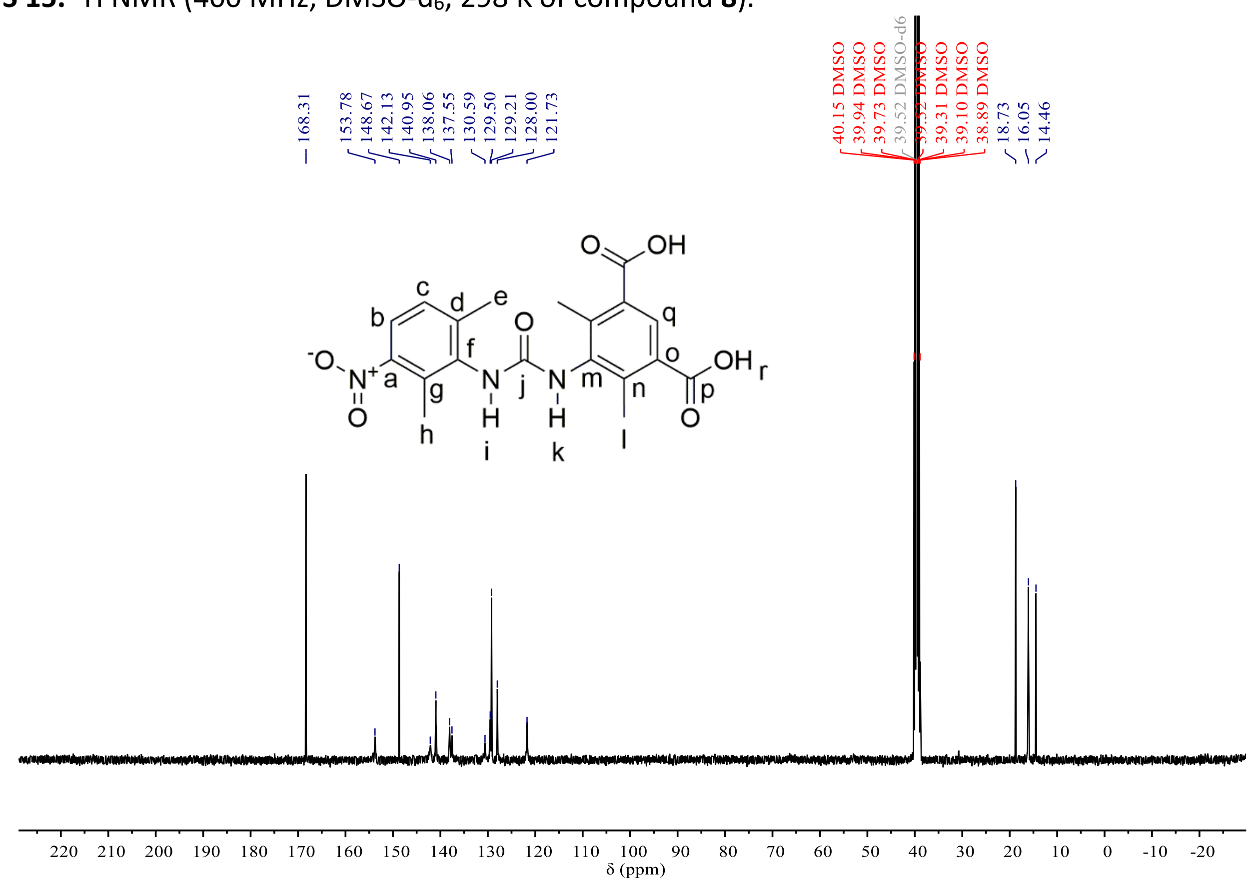

Figure S 16. ^{13}C{H} (100 MHz, DMSO-d6, 298 K of compound **8**).

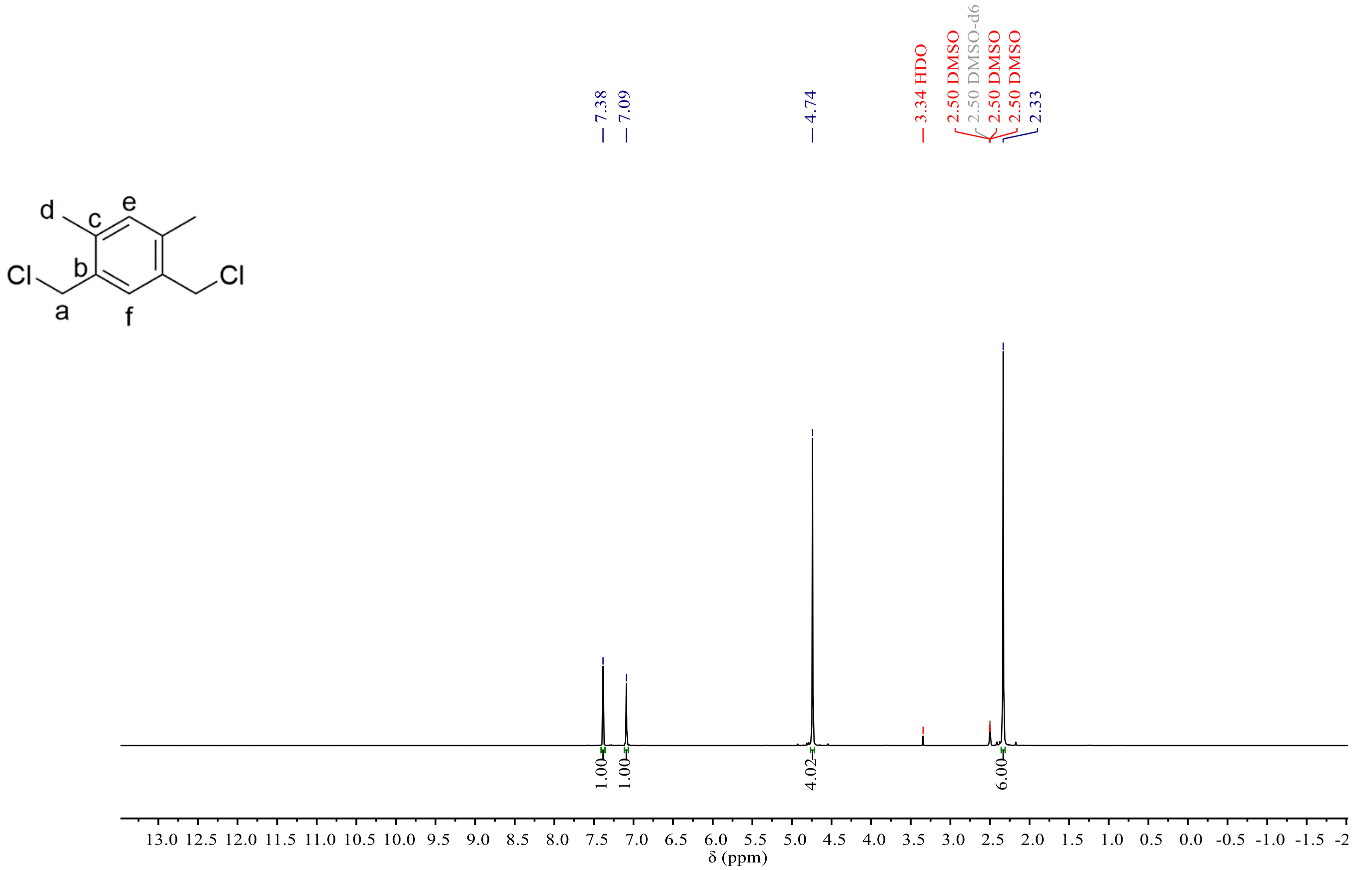

Figure S 17. ^{1}H NMR (400 MHz, DMSO-d$_6$, 298 K of compound **9**).

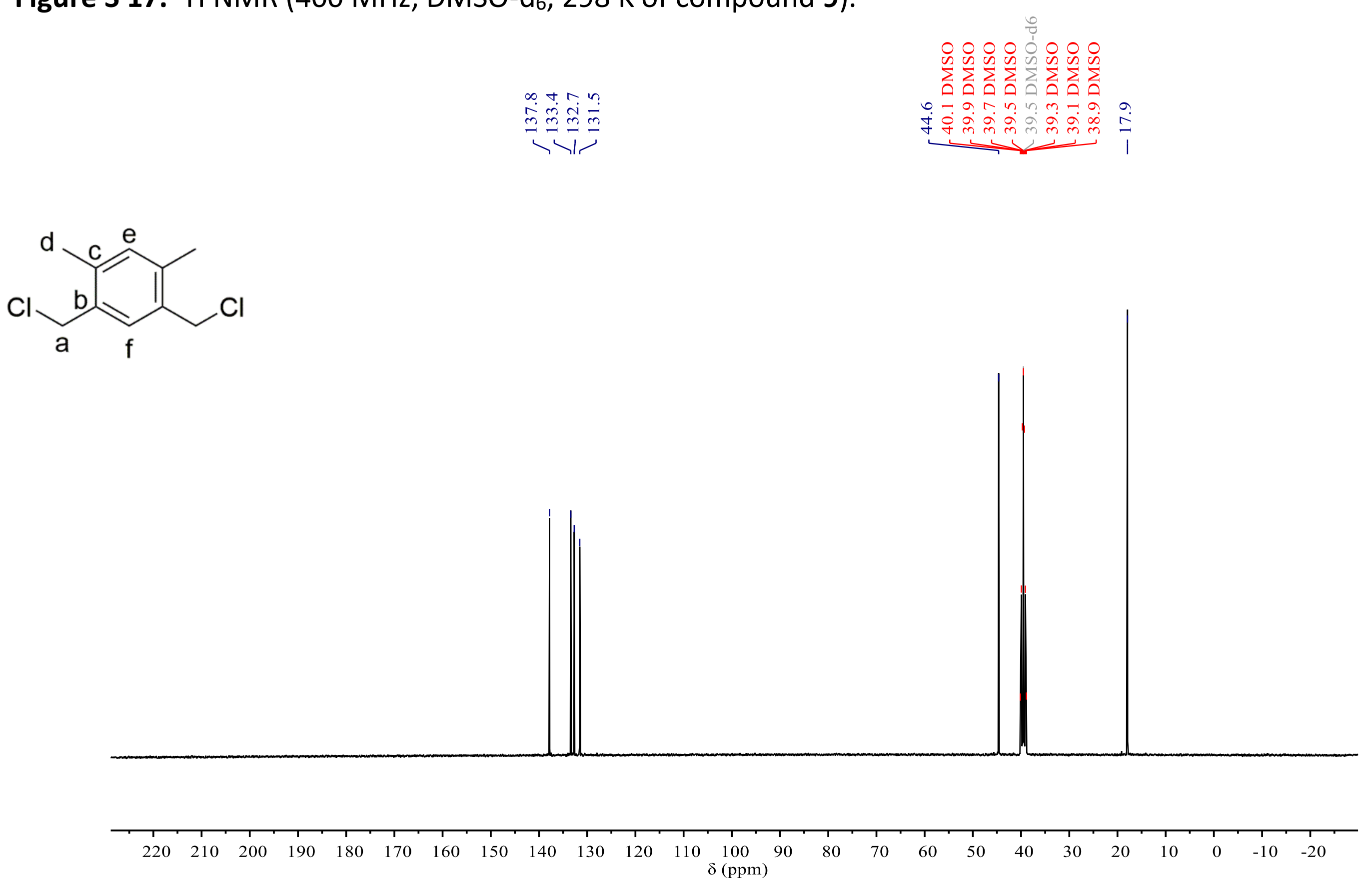

Figure S 18. $^{13}C\{H\}$ (100 MHz, DMSO-d$_6$, 298 K of compound **9**).

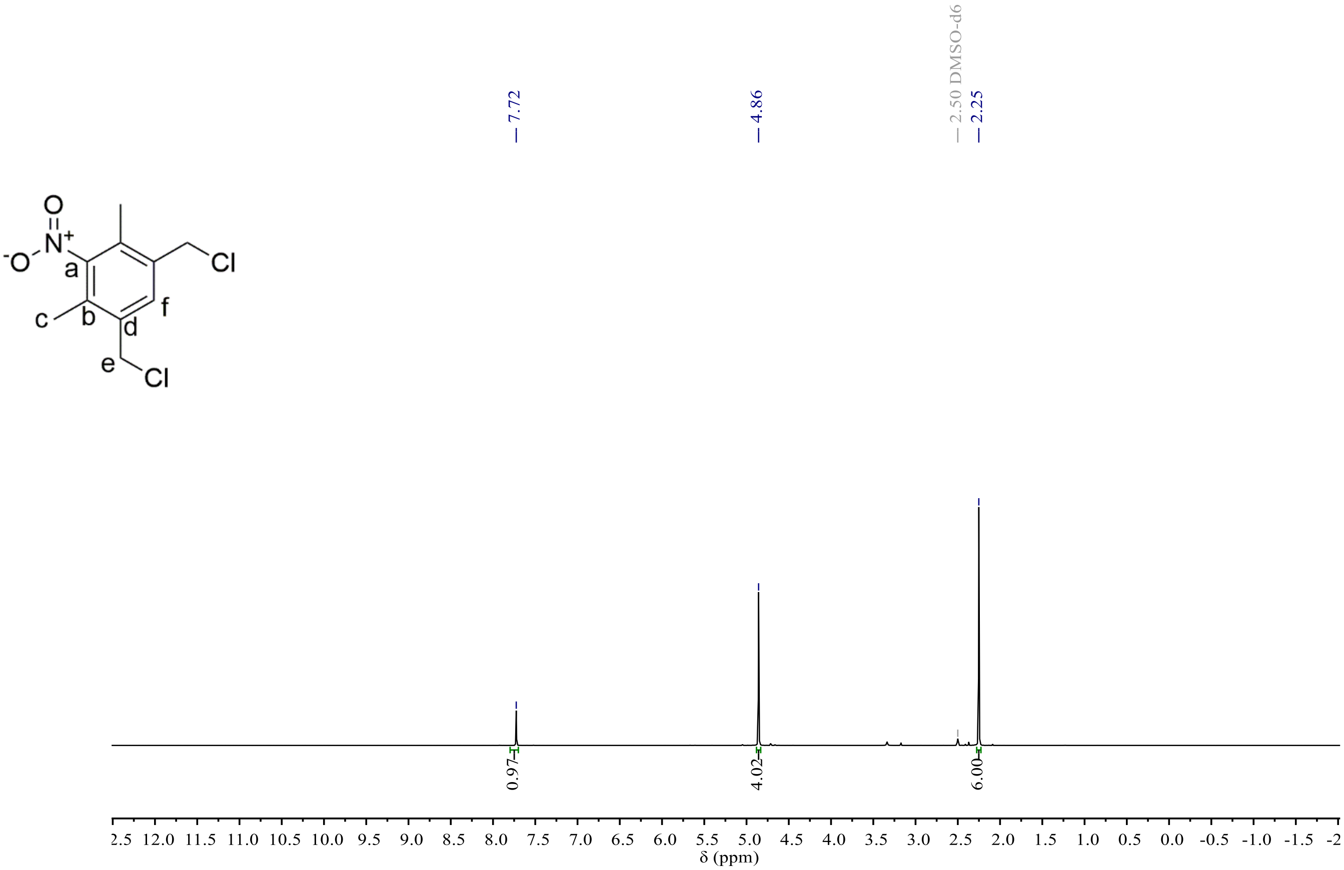

Figure S 19. ^{1}H NMR (400 MHz, DMSO-d$_6$, 298 K of compound **10**).

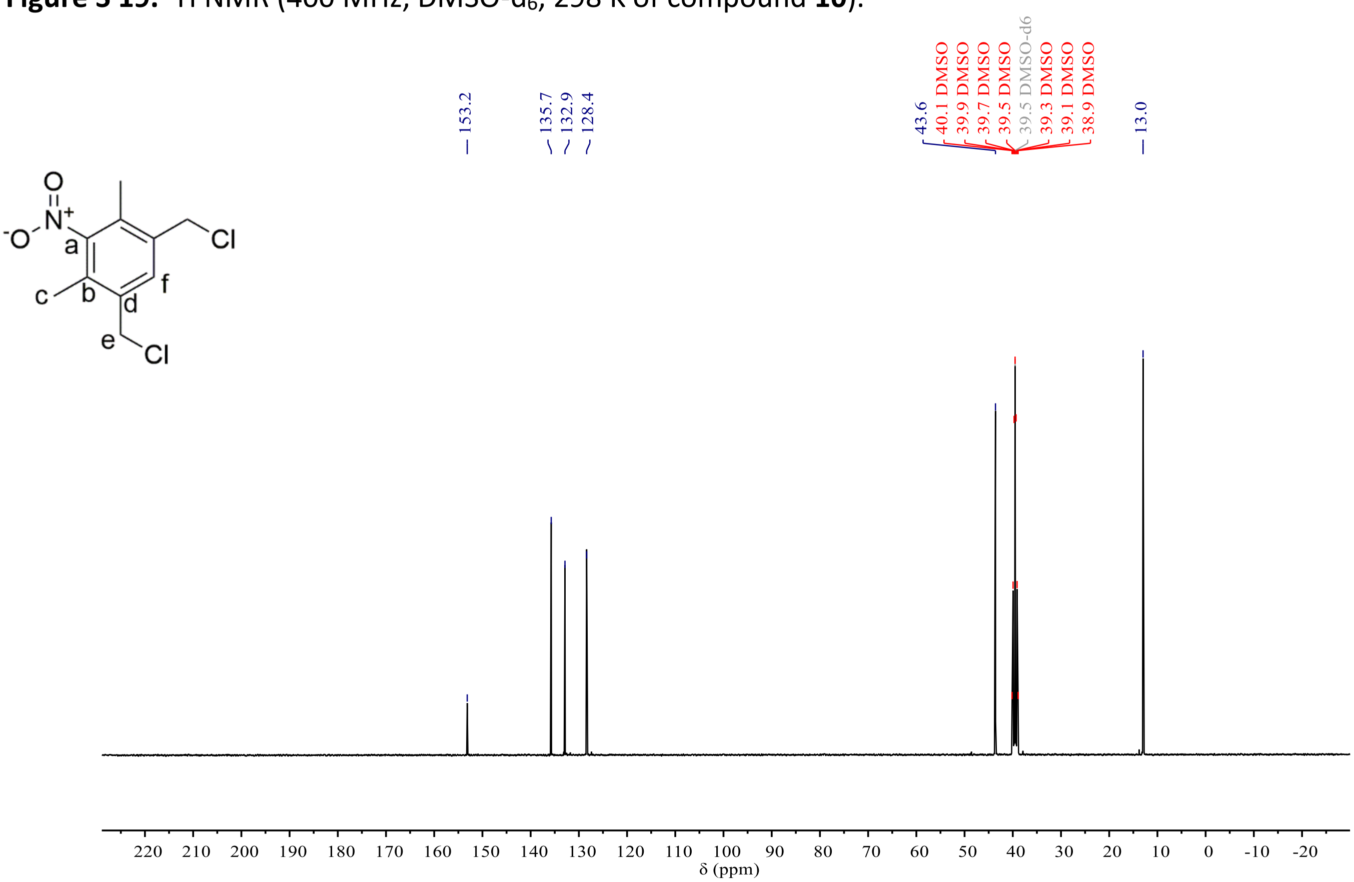

Figure S 20. ^{13}C{H}(100 MHz, DMSO-d$_6$, 298 K of compound **10**).

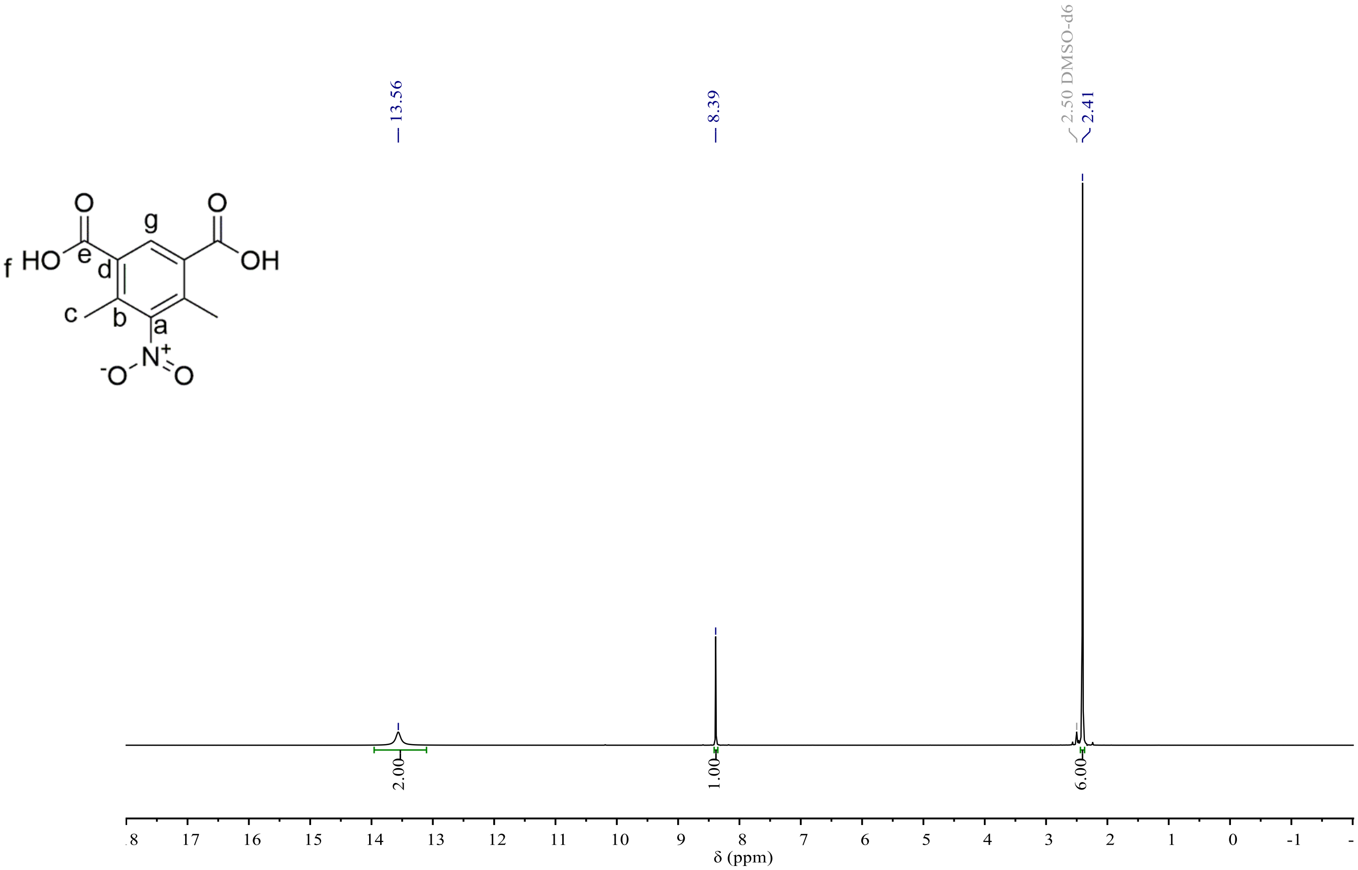

Figure S 21. ^{1}H NMR (400 MHz, DMSO-d$_6$, 298 K of compound **11**).

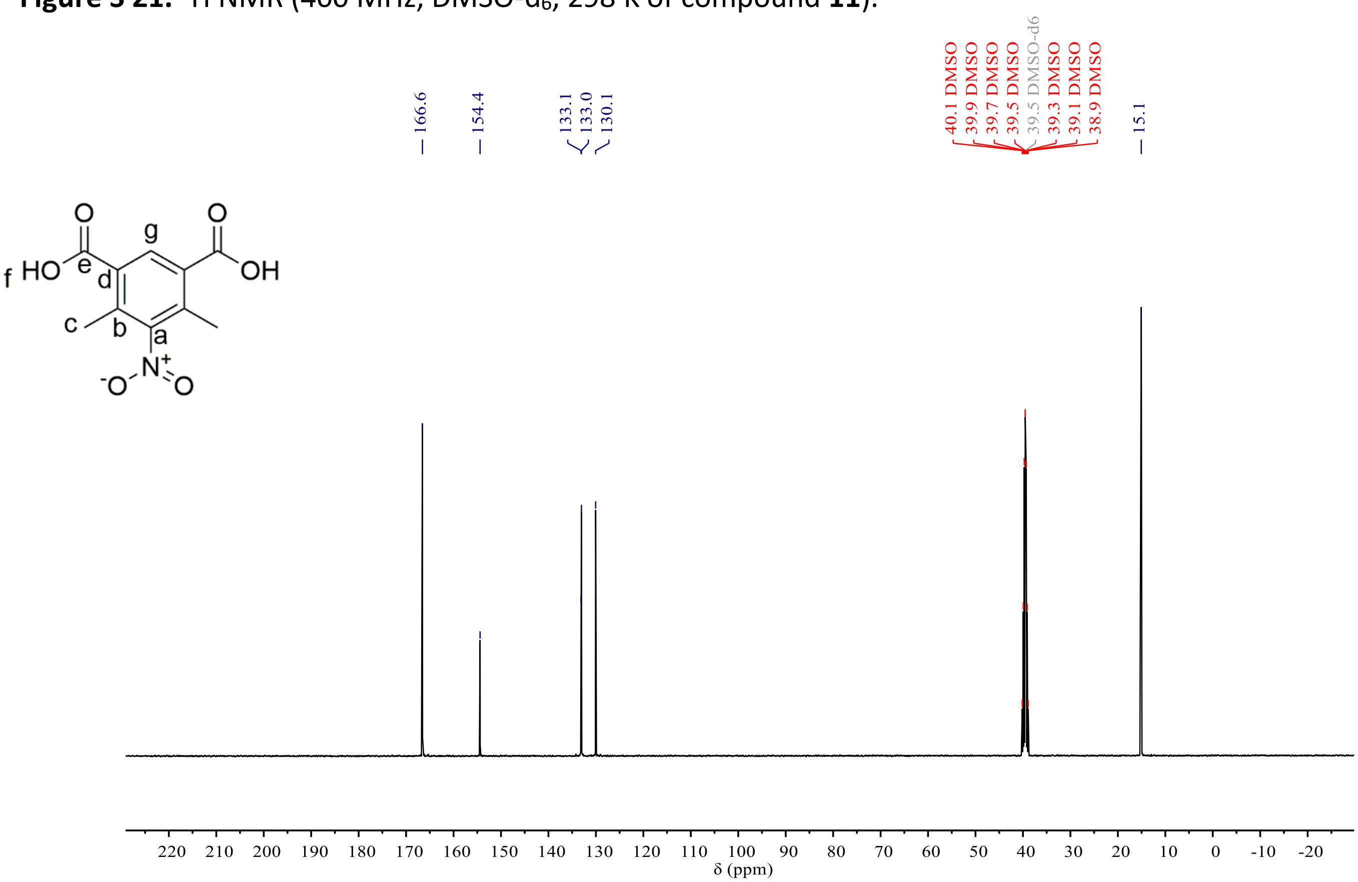

Figure S 22. ^{13}C{H} (100 MHz, DMSO-d$_6$, 298 K of compound **11**).

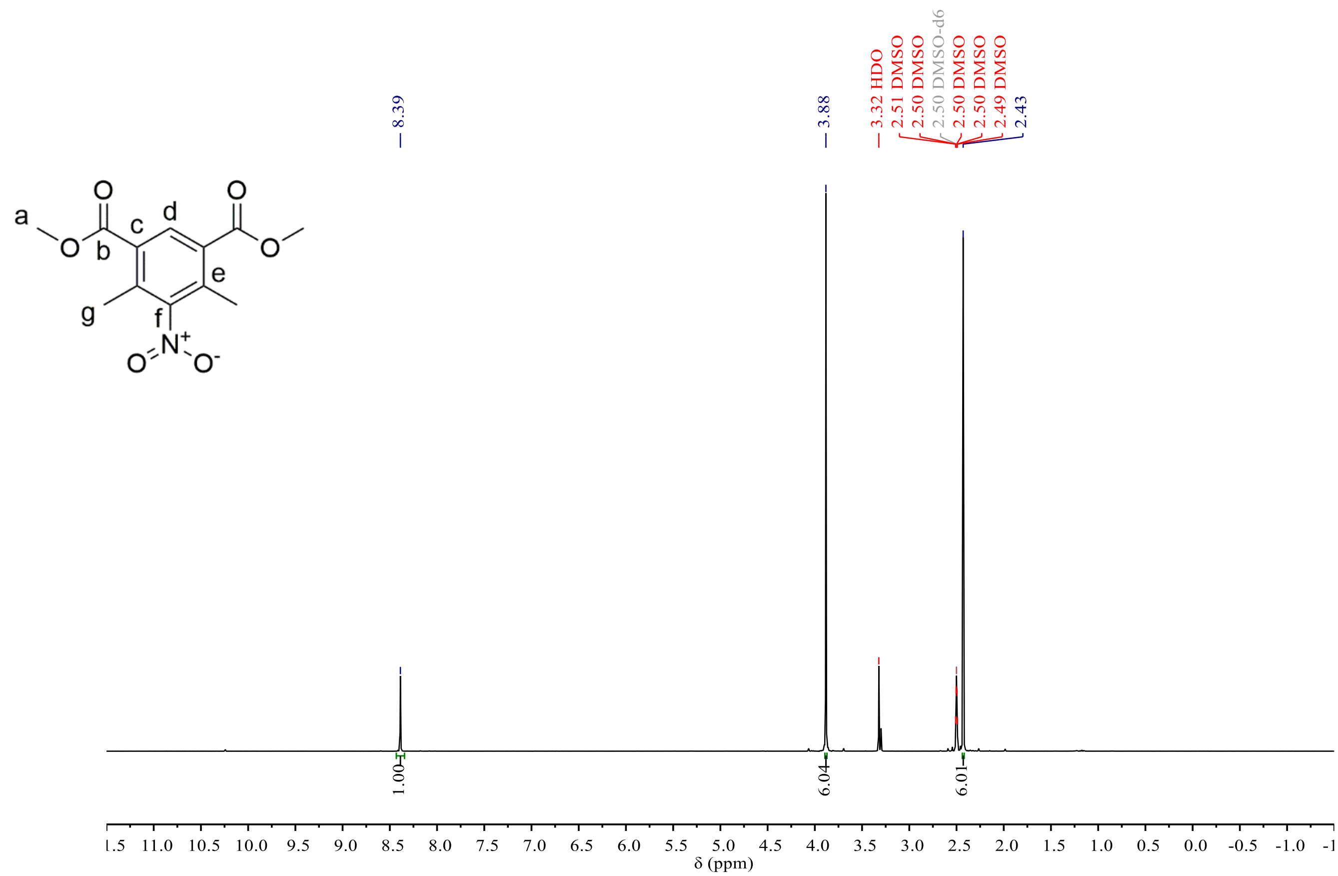

Figure S 23. ^{1}H NMR (400 MHz, DMSO-d$_6$, 298 K of compound **12**).

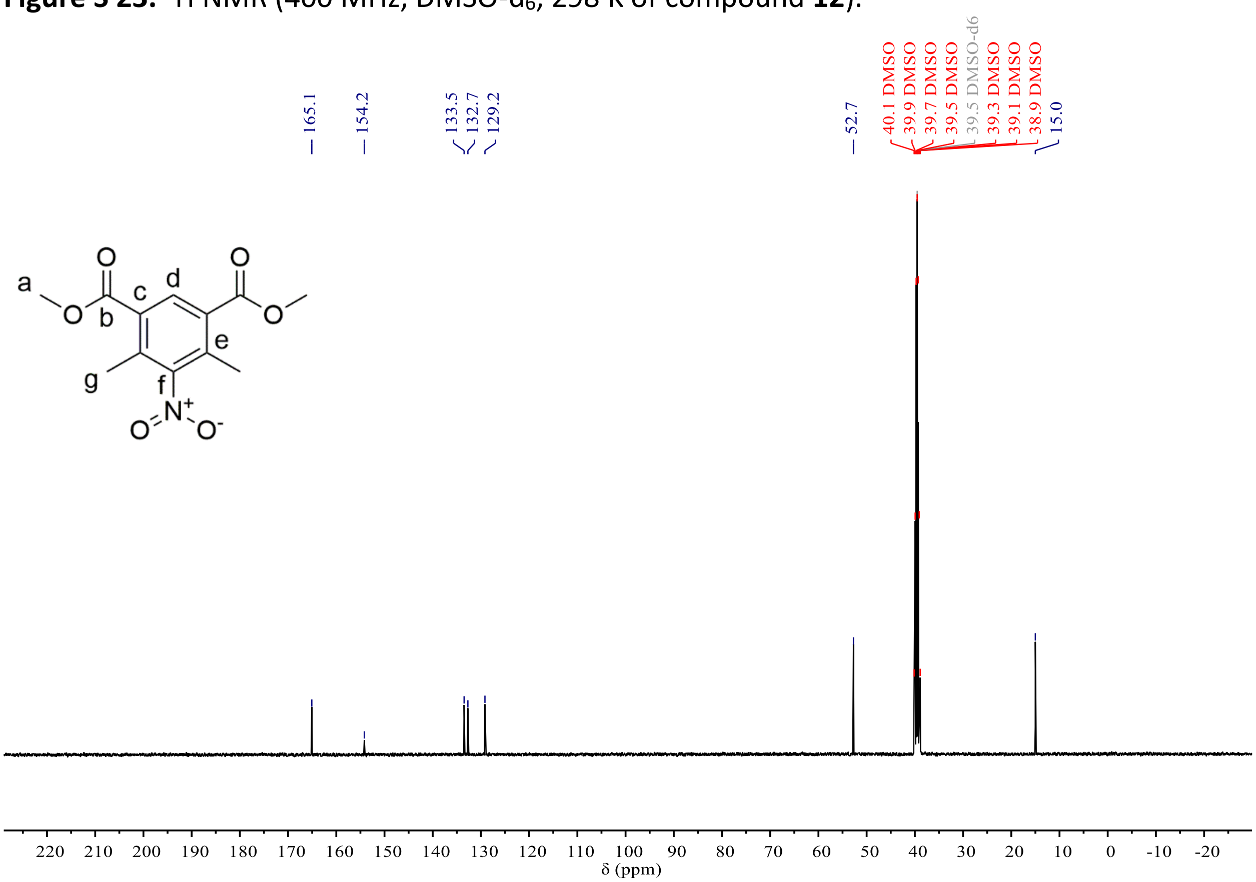

Figure S 24. ^{13}C{H} (100 MHz, DMSO-d$_6$, 298 K of compound **12**).

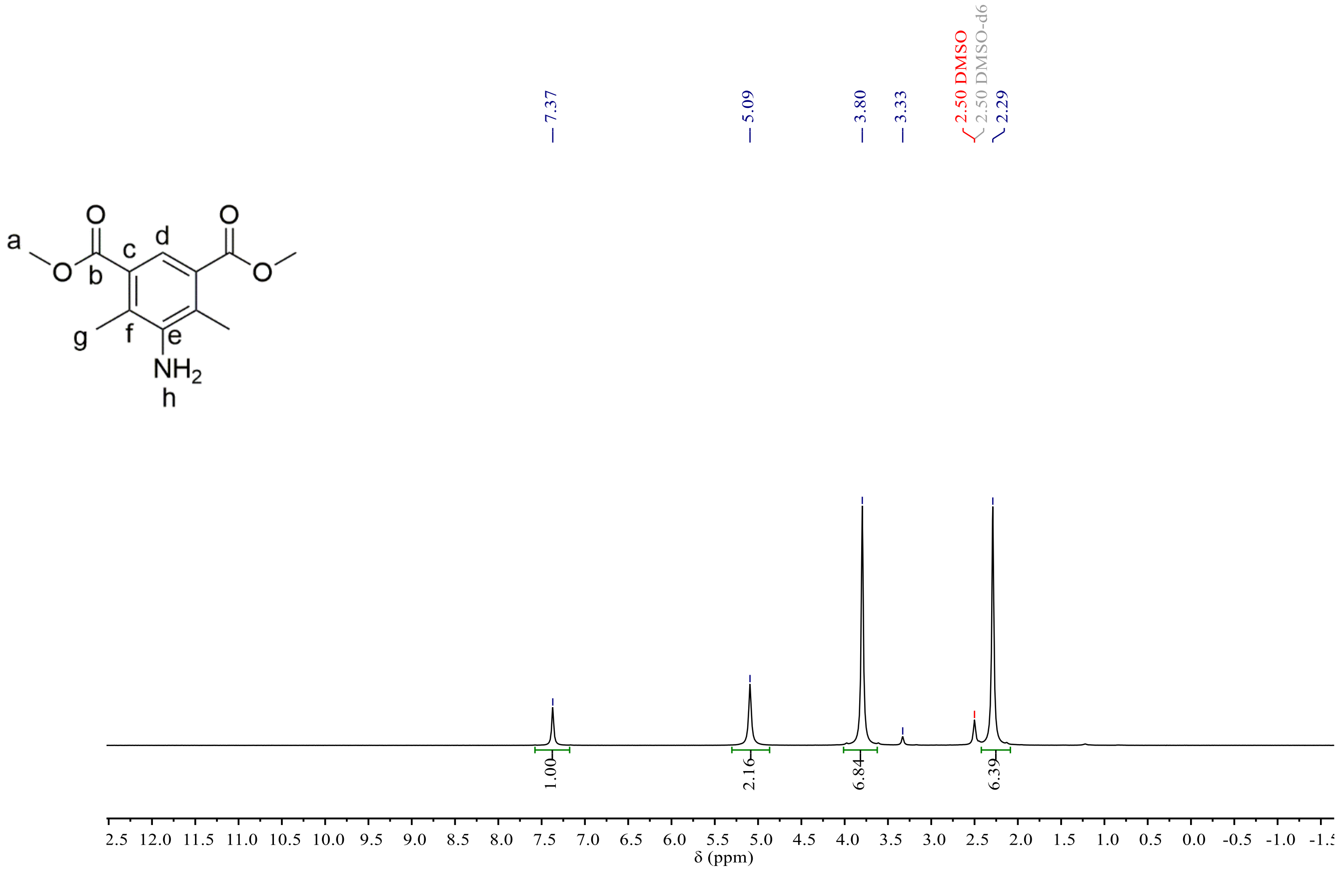

Figure S 25. ^{1}H NMR (400 MHz, DMSO-d$_6$, 298 K of compound **13**).

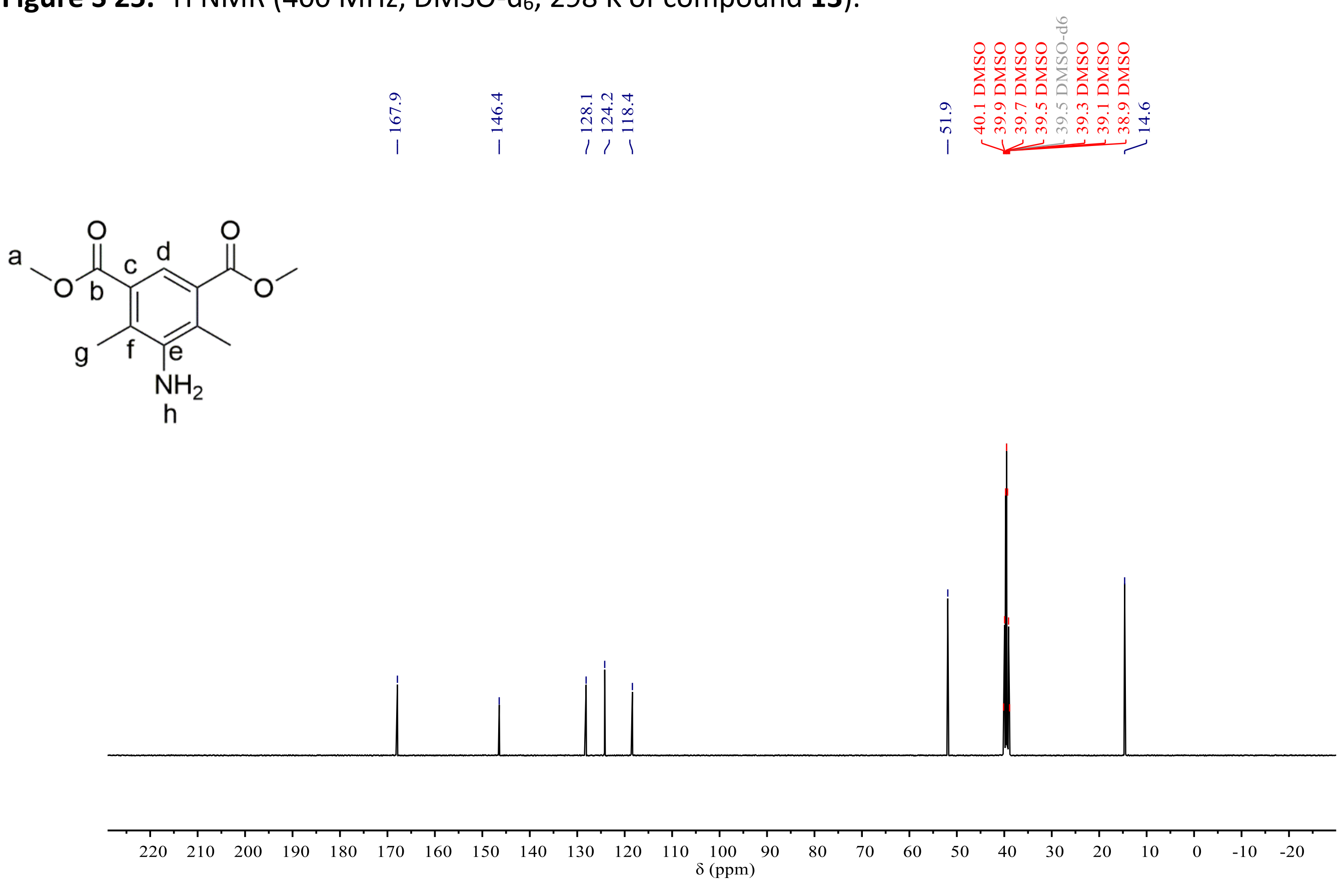

Figure S 26. ^{13}C{H} (100 MHz, DMSO-d6, 298 K of compound **13**).

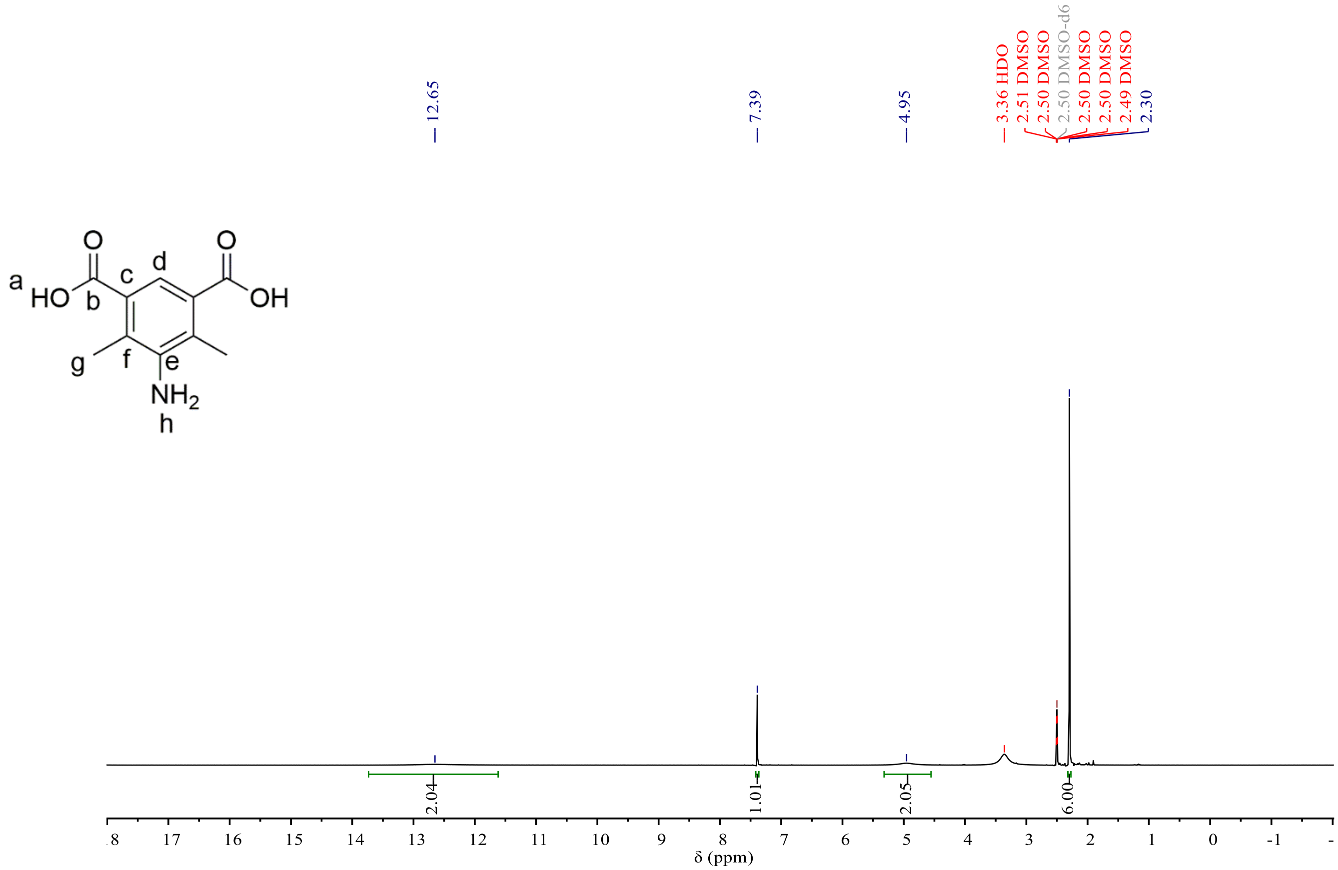

Figure S 27. ^{1}H NMR (400 MHz, DMSO-d_6, 298 K of compound **14**).

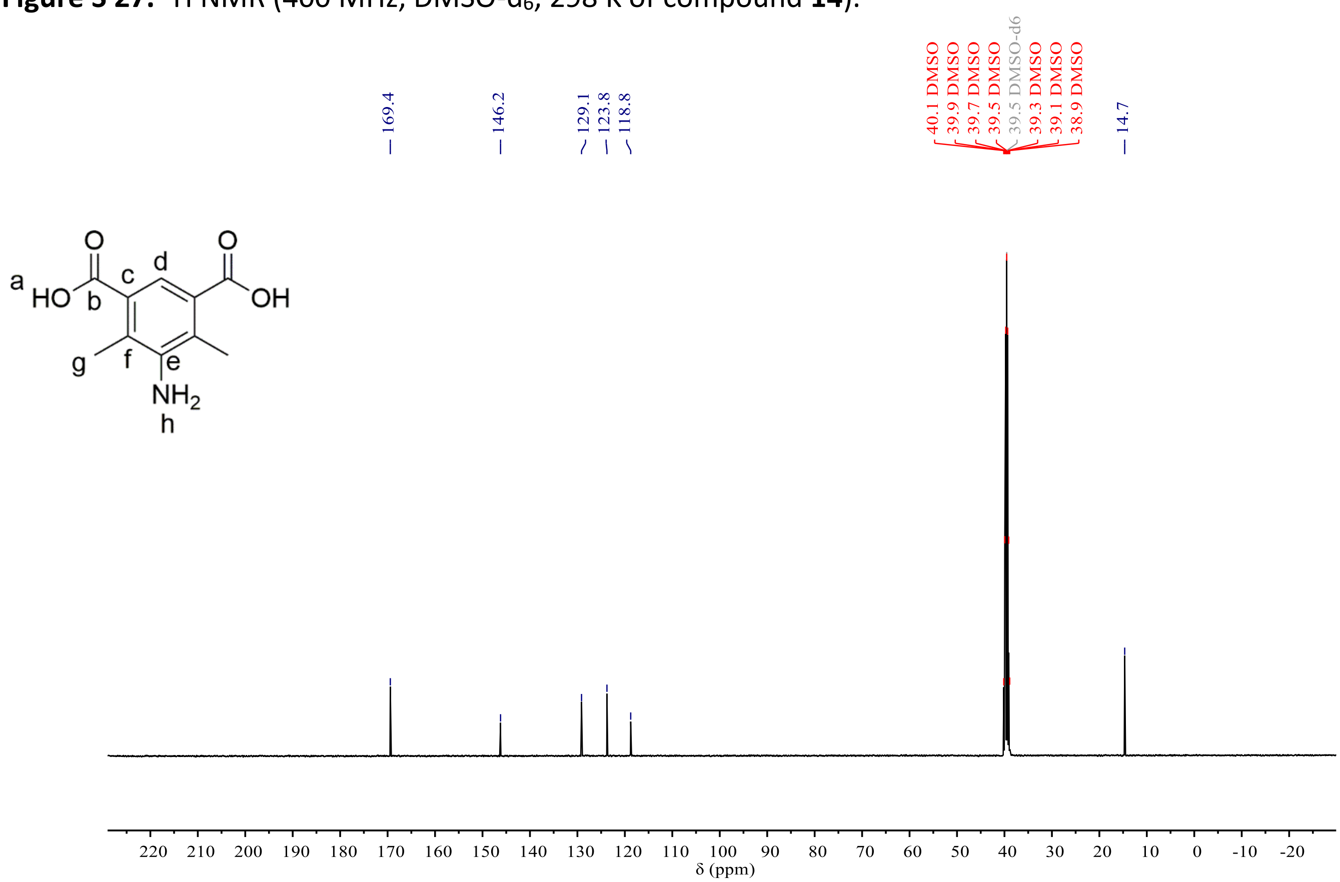

Figure S 28. ^{13}C{H} (100 MHz, DMSO-d_6, 298 K of compound **14**).

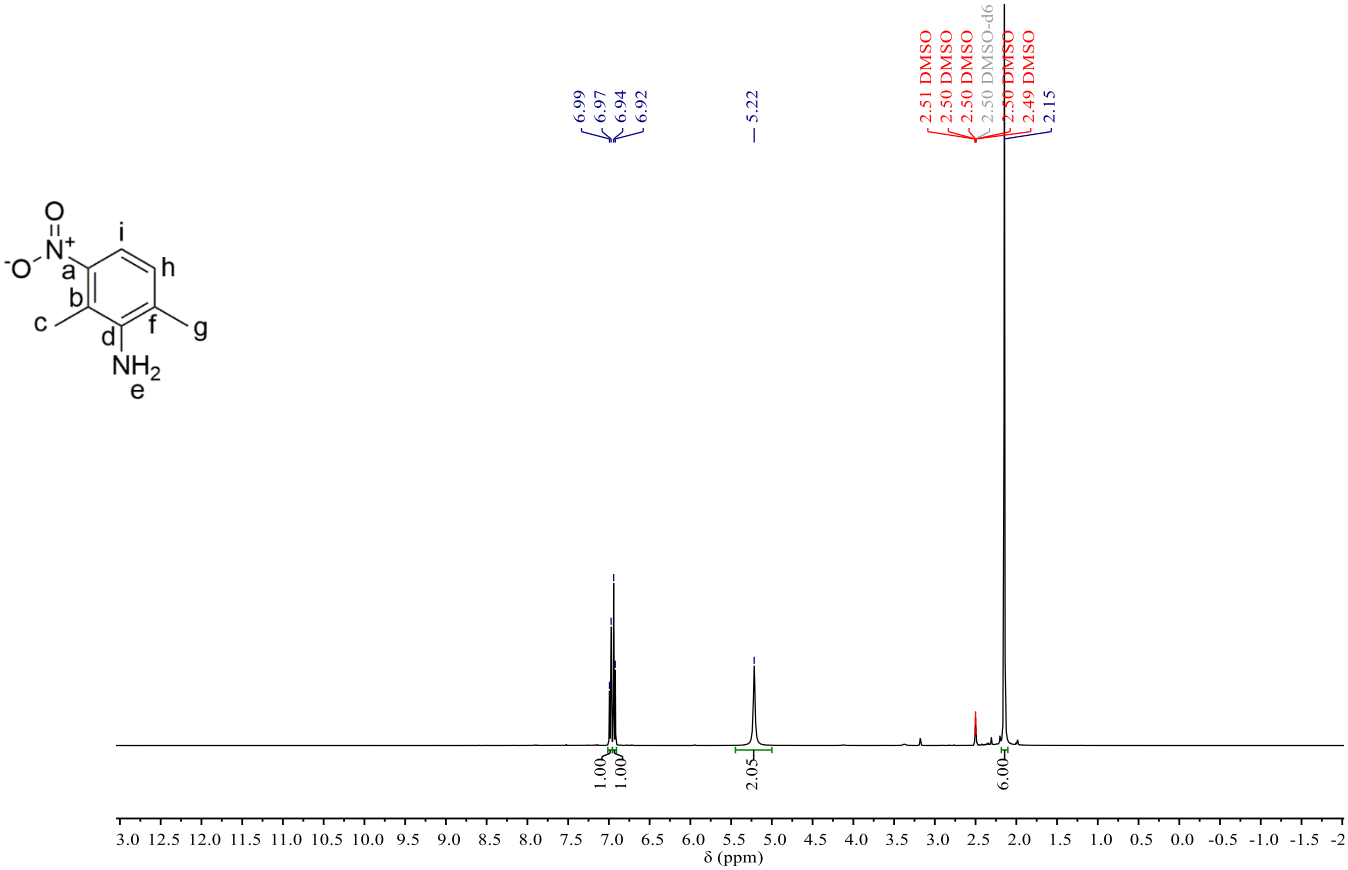

Figure S 29. ^{1}H NMR (400 MHz, DMSO-d_6, 298 K of compound **15**).

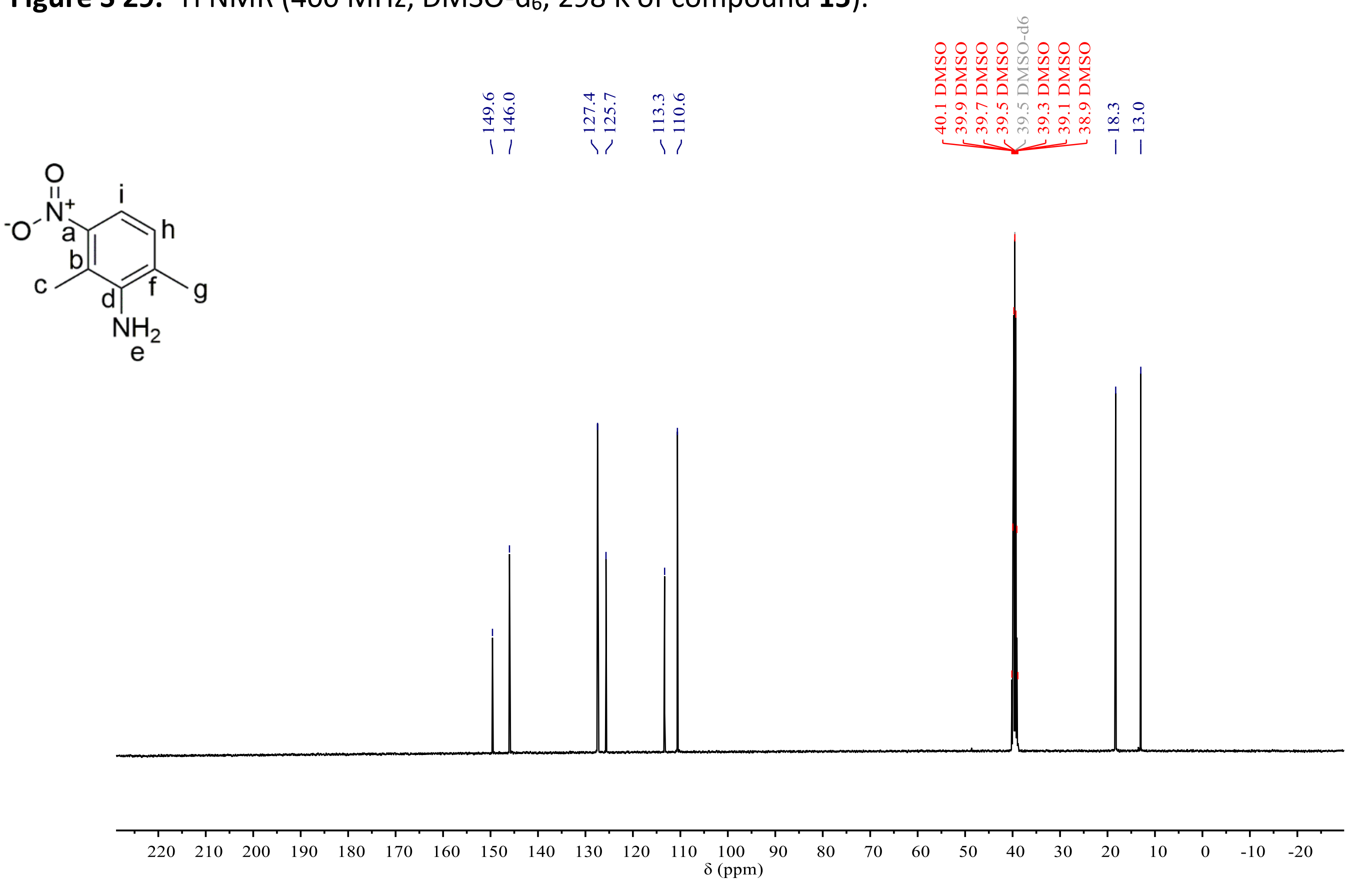

Figure S 30. ^{13}C{H} (100 MHz, DMSO-d_6, 298 K of compound **15**).

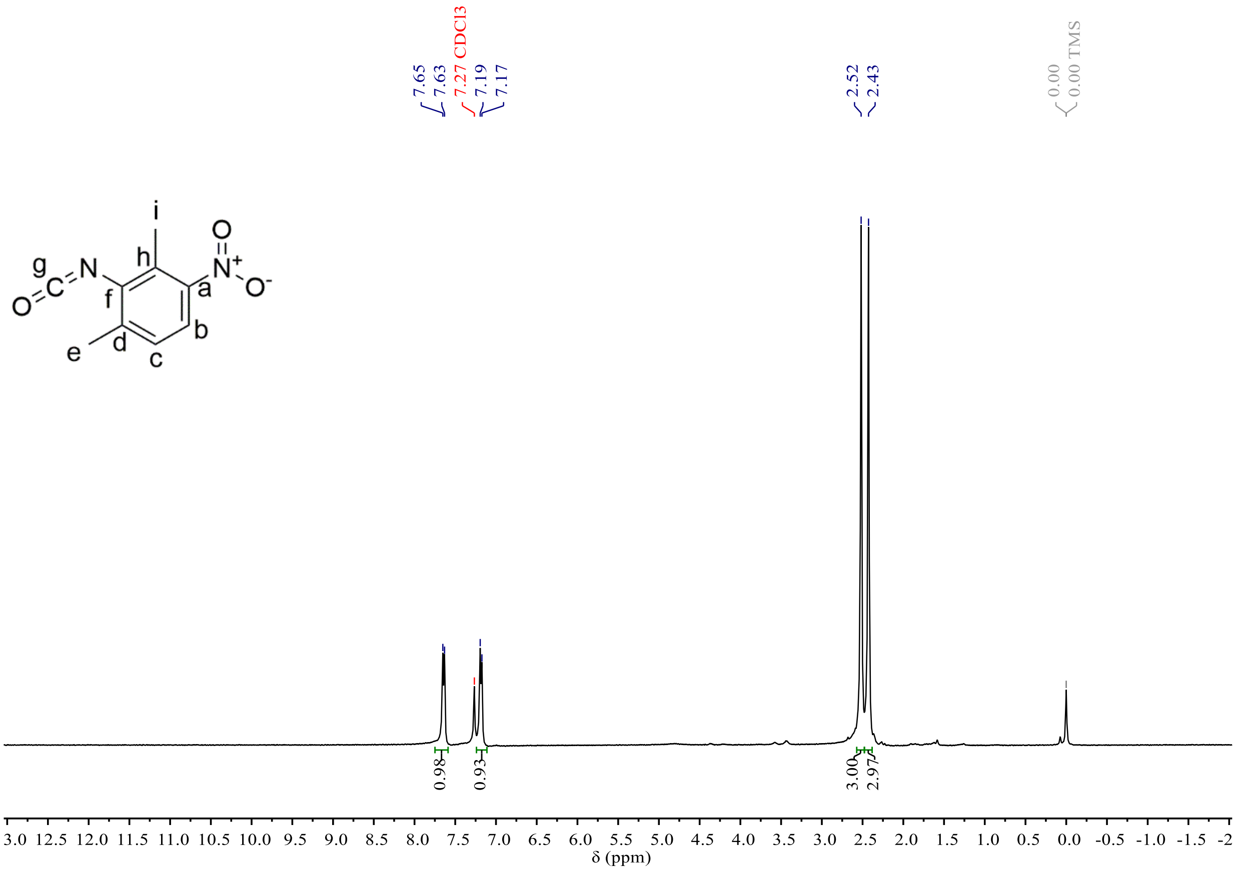

Figure S 31. ^{1}H NMR (400 MHz, DMSO-d$_6$, 298 K of compound **16**).

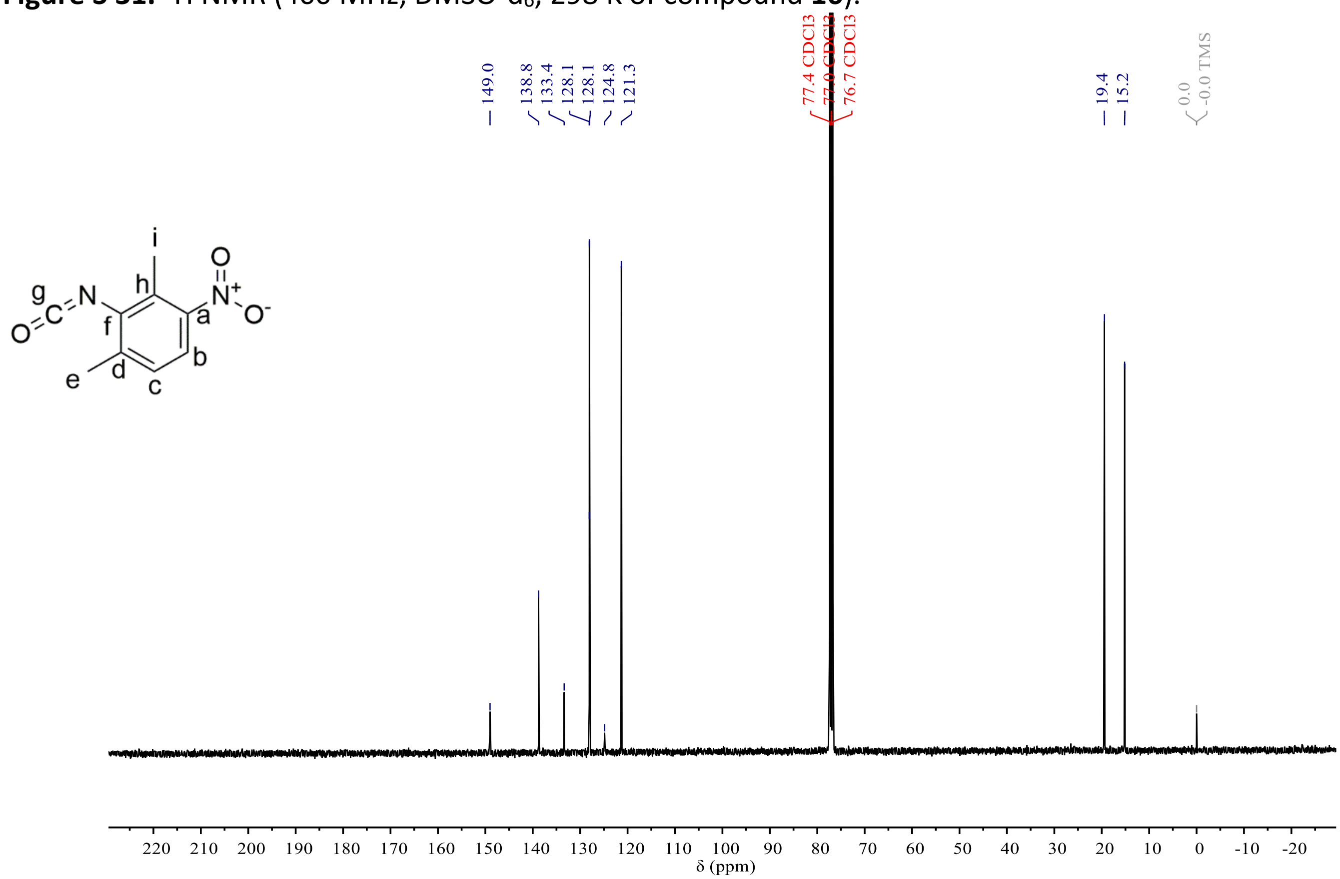

Figure S 32. $^{13}C\{H\}$ (100 MHz, DMSO-d$_6$, 298 K of compound **16**).

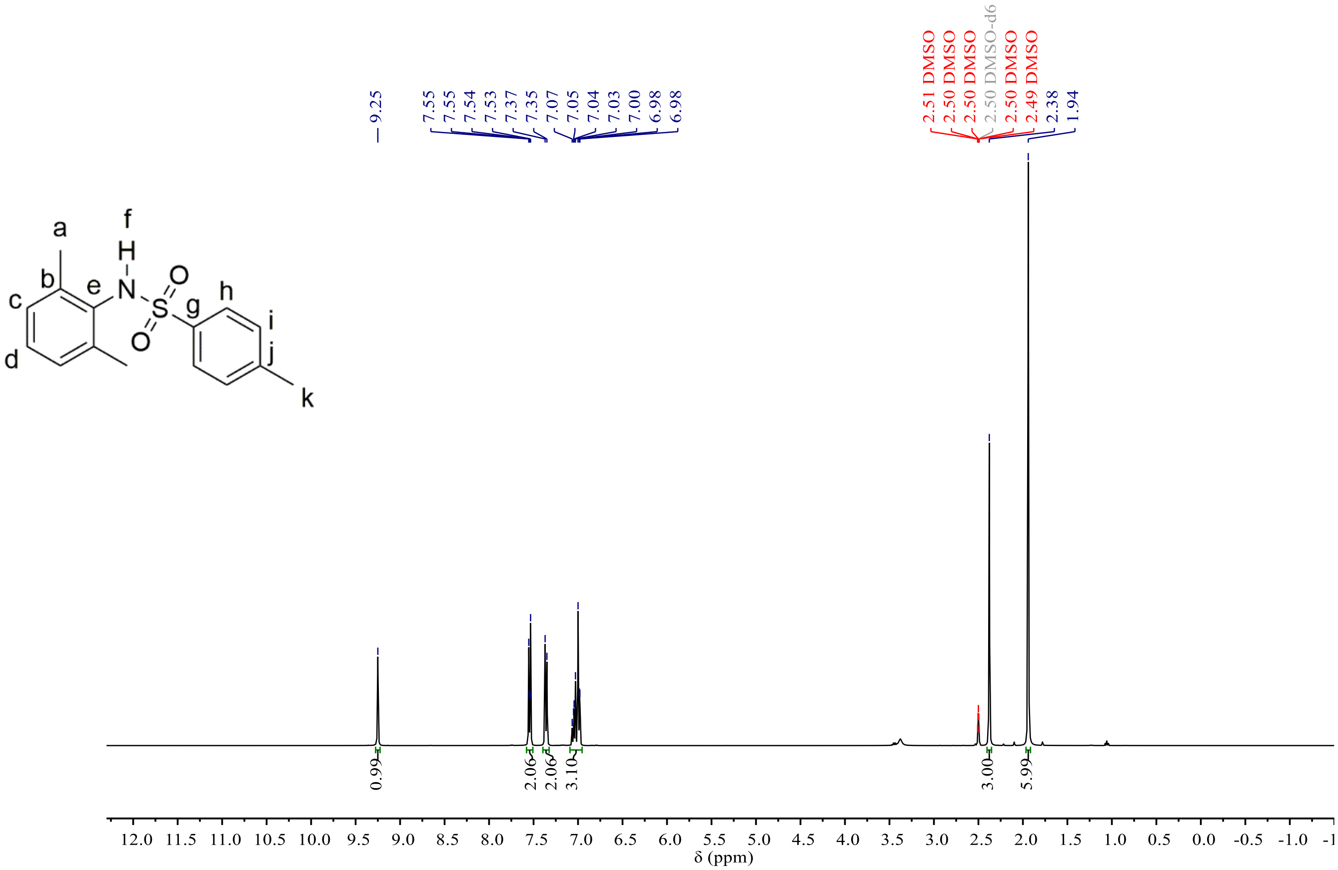

Figure S 33. ^{1}H NMR (400 MHz, DMSO-d$_6$, 298 K of compound **17**).

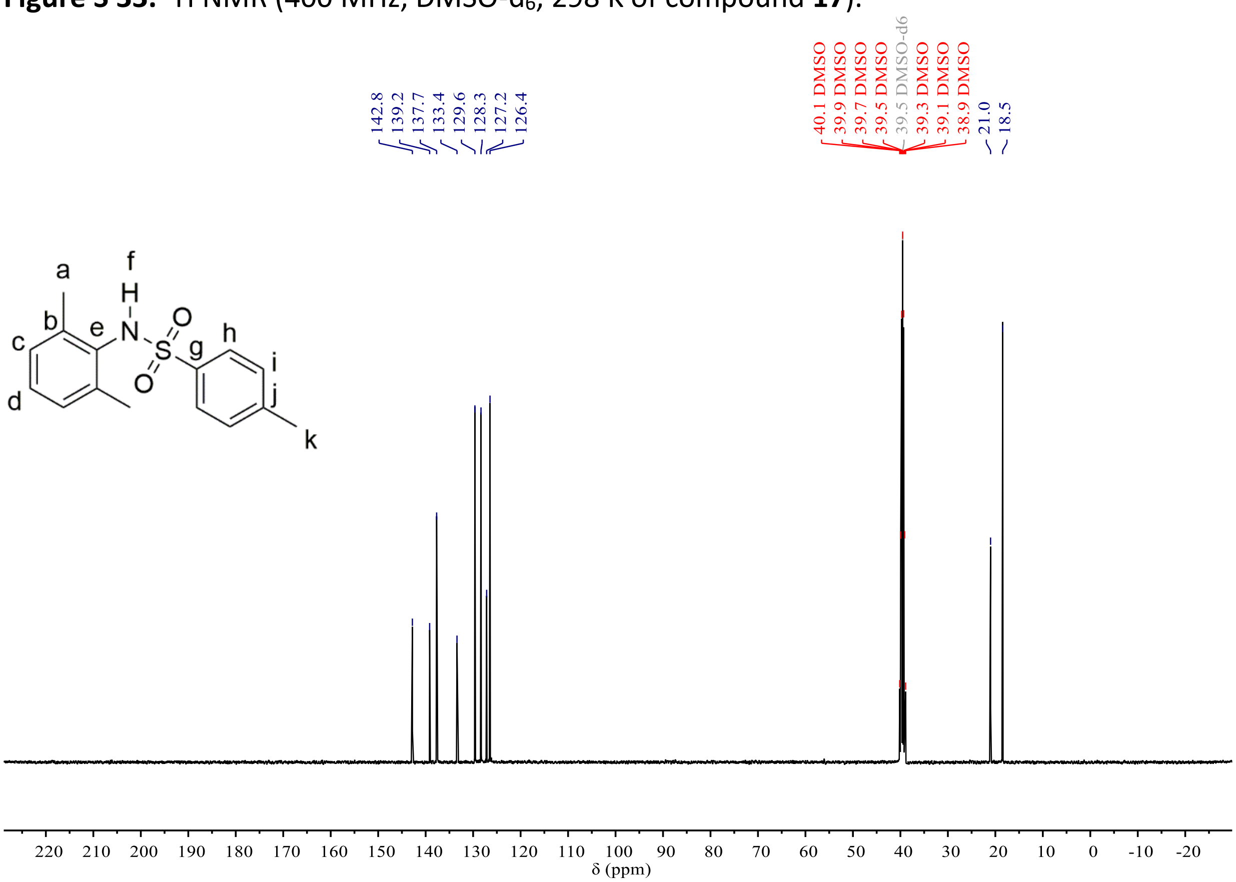

Figure S 34. ^{13}C{H} (100 MHz, DMSO-d6, 298 K of compound **17**).

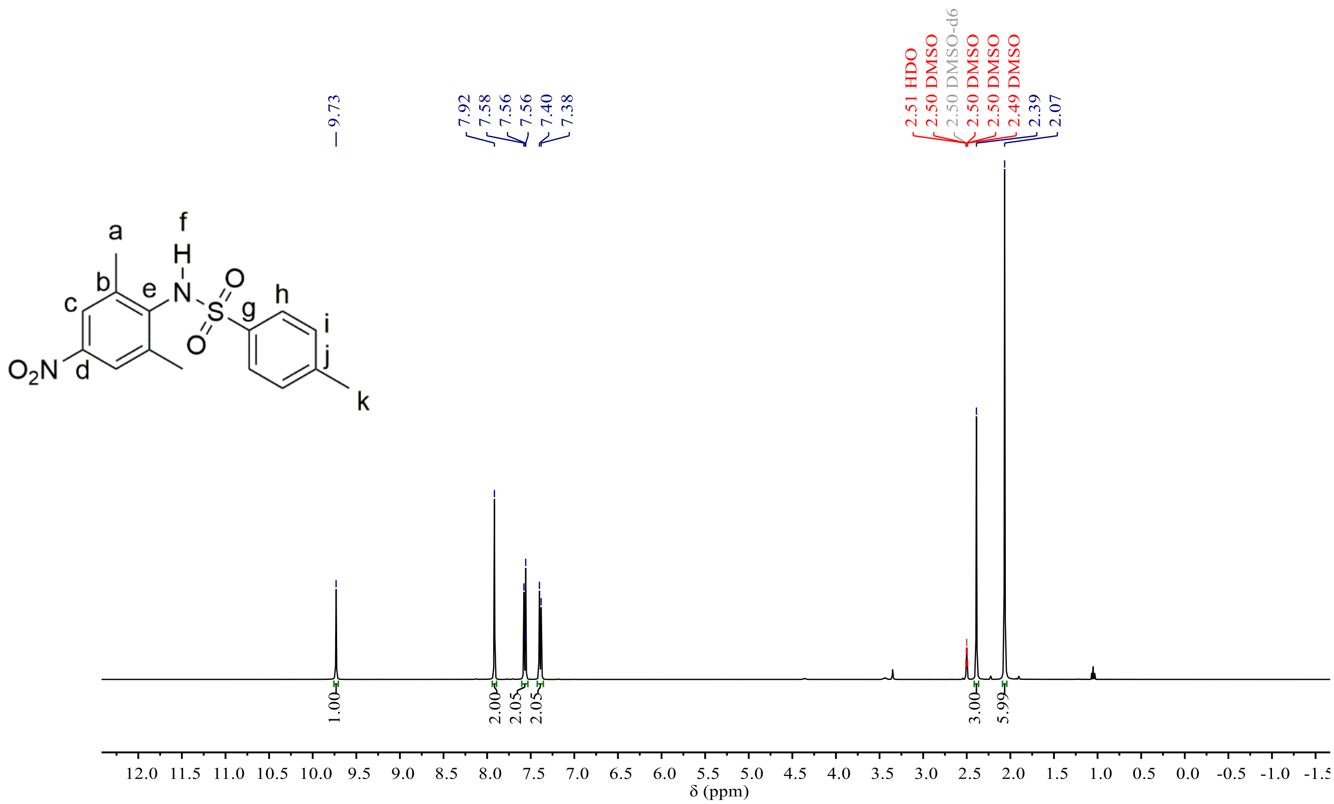

Figure S 35. ^{1}H NMR (400 MHz, DMSO-d_6, 298 K of compound **18**).

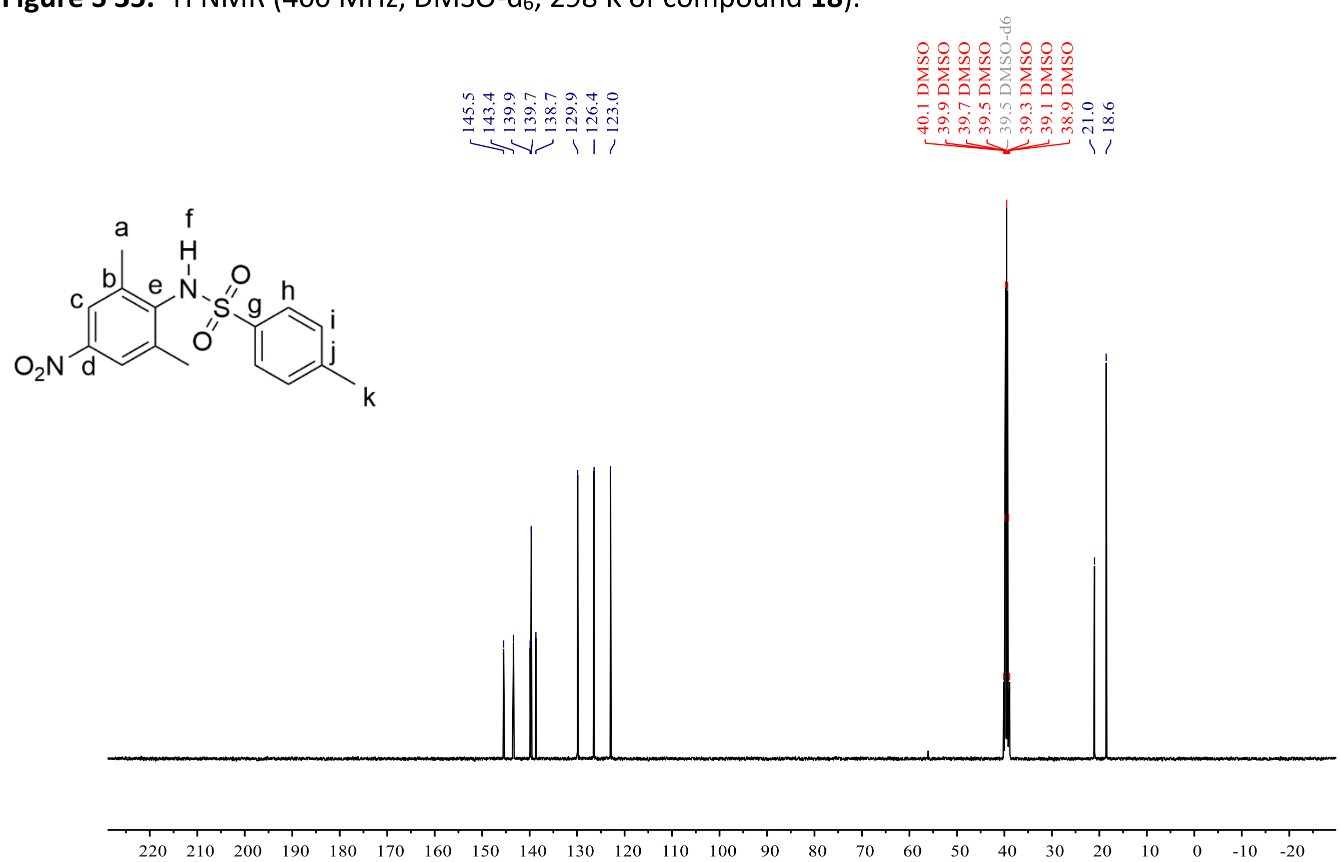

Figure S 36. $^{13}C\{H\}$ (100 MHz, DMSO-d_6, 298 K of compound **18**).

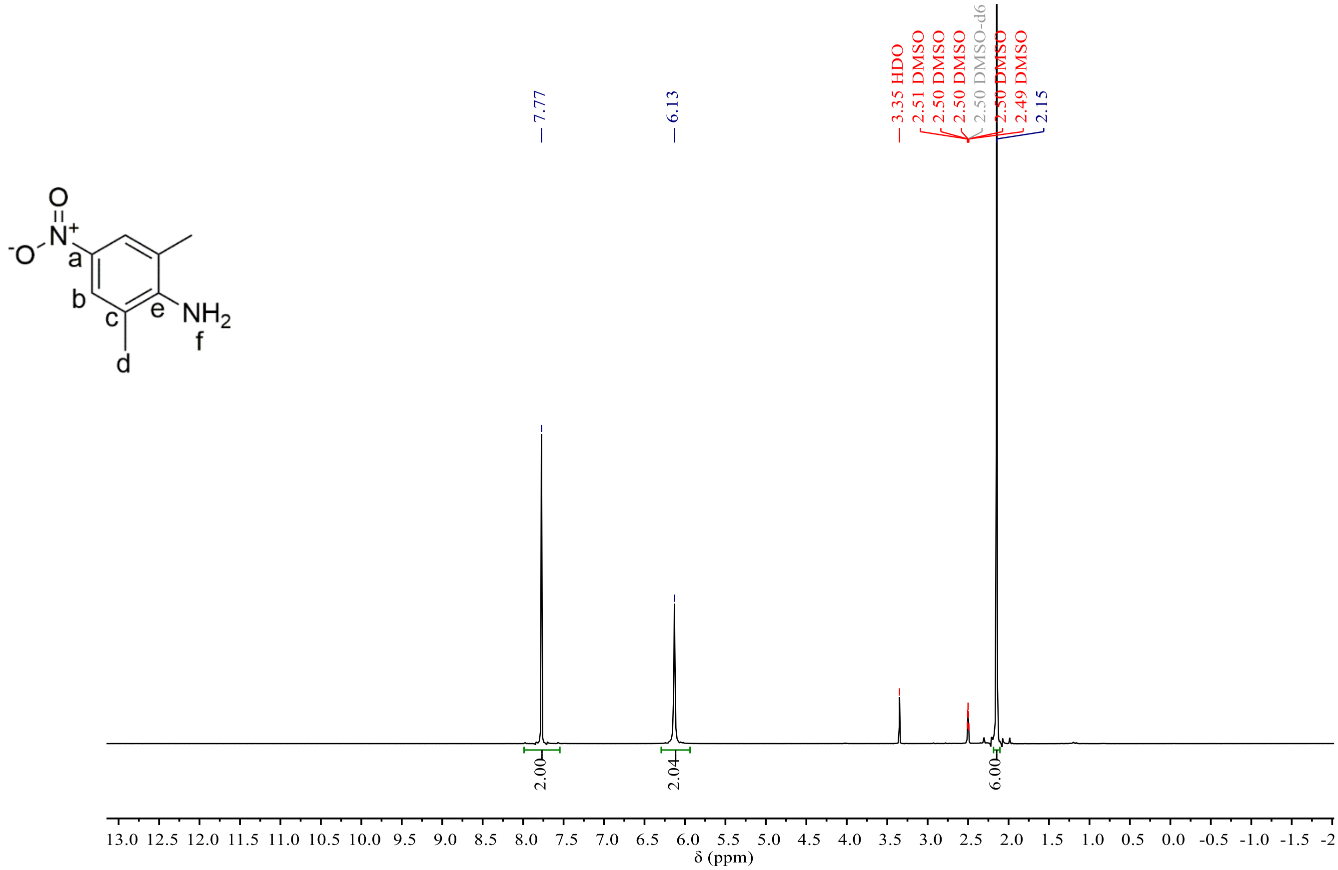

Figure S 37. ^{1}H NMR (400 MHz, DMSO-d$_6$, 298 K of compound **19**).

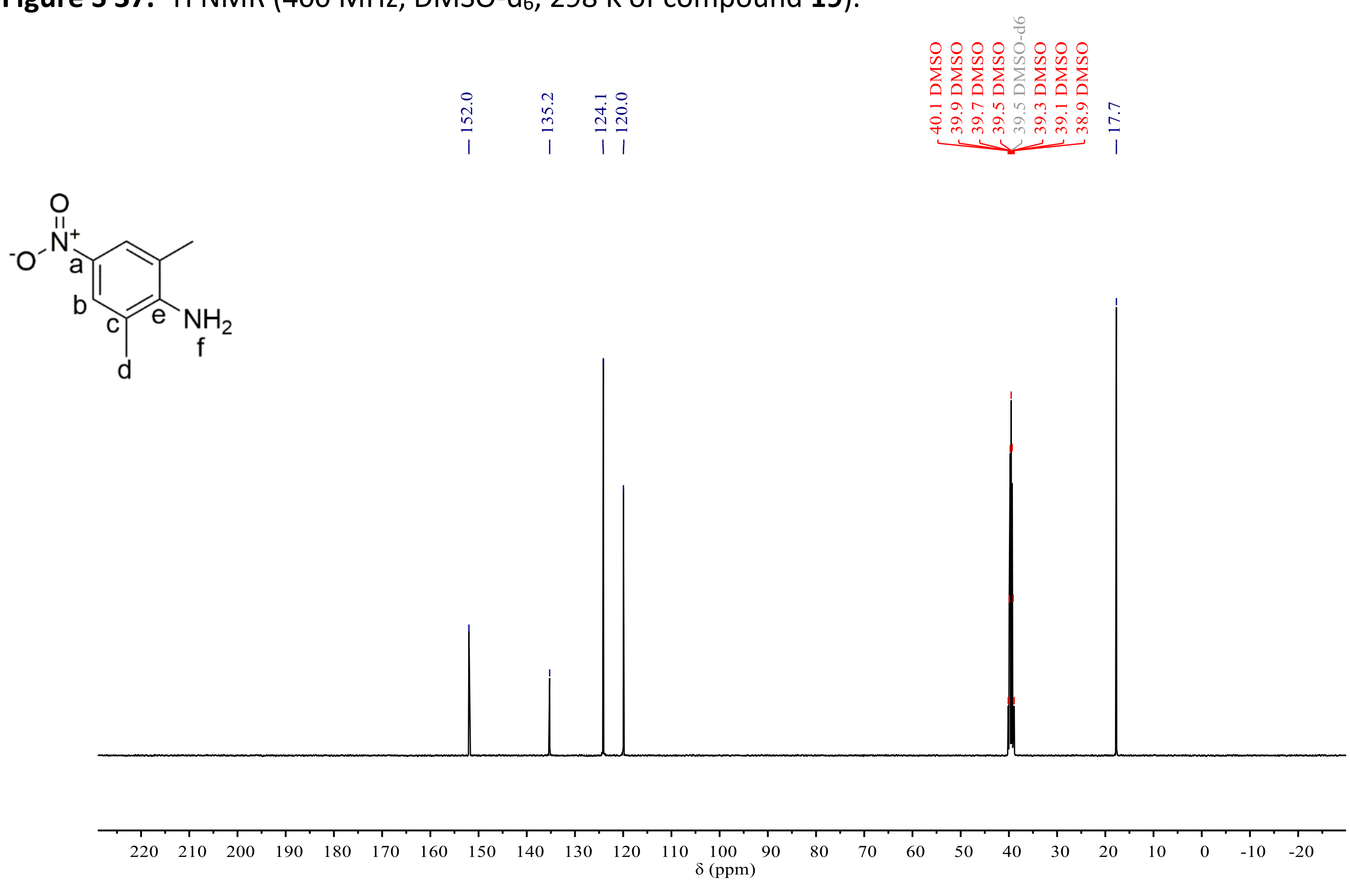

Figure S 38. ^{13}C{H} (100 MHz, DMSO-d$_6$, 298 K of compound **19**).

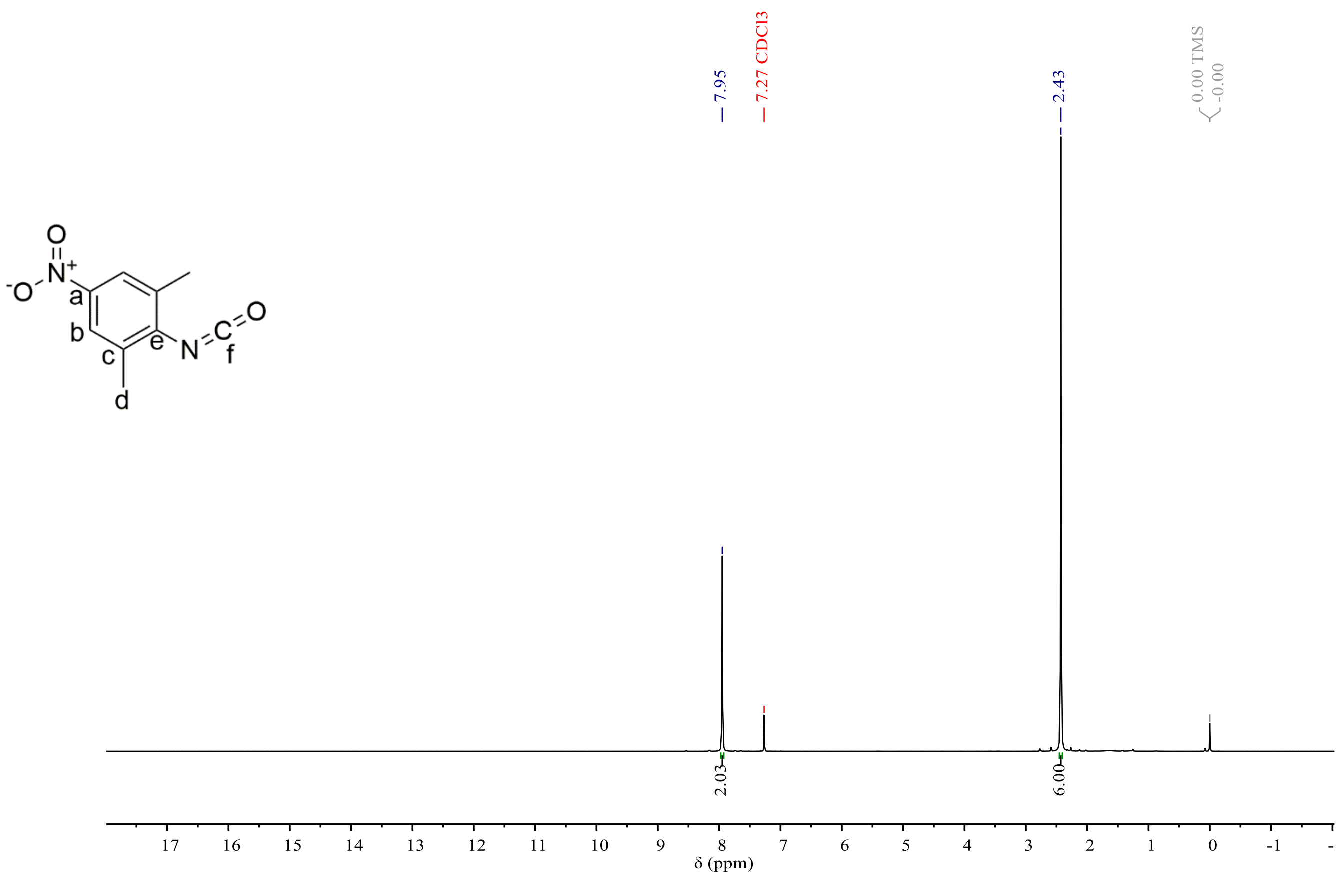

Figure S 39. ^{1}H NMR (400 MHz, DMSO-d$_6$, 298 K of compound **20**).

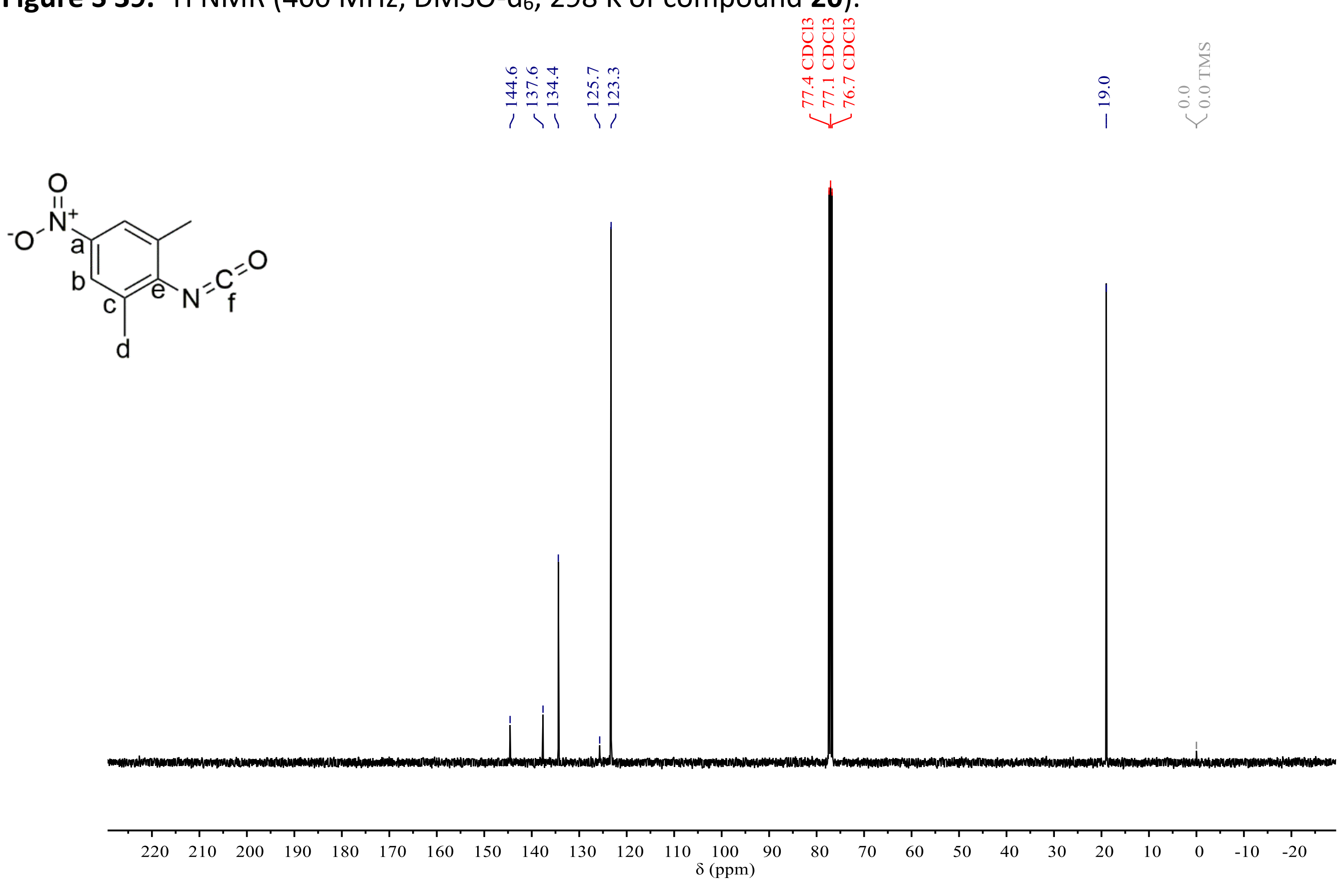

Figure S 40. ^{13}C{H} (100 MHz, DMSO-d$_6$, 298 K of compound **20**).

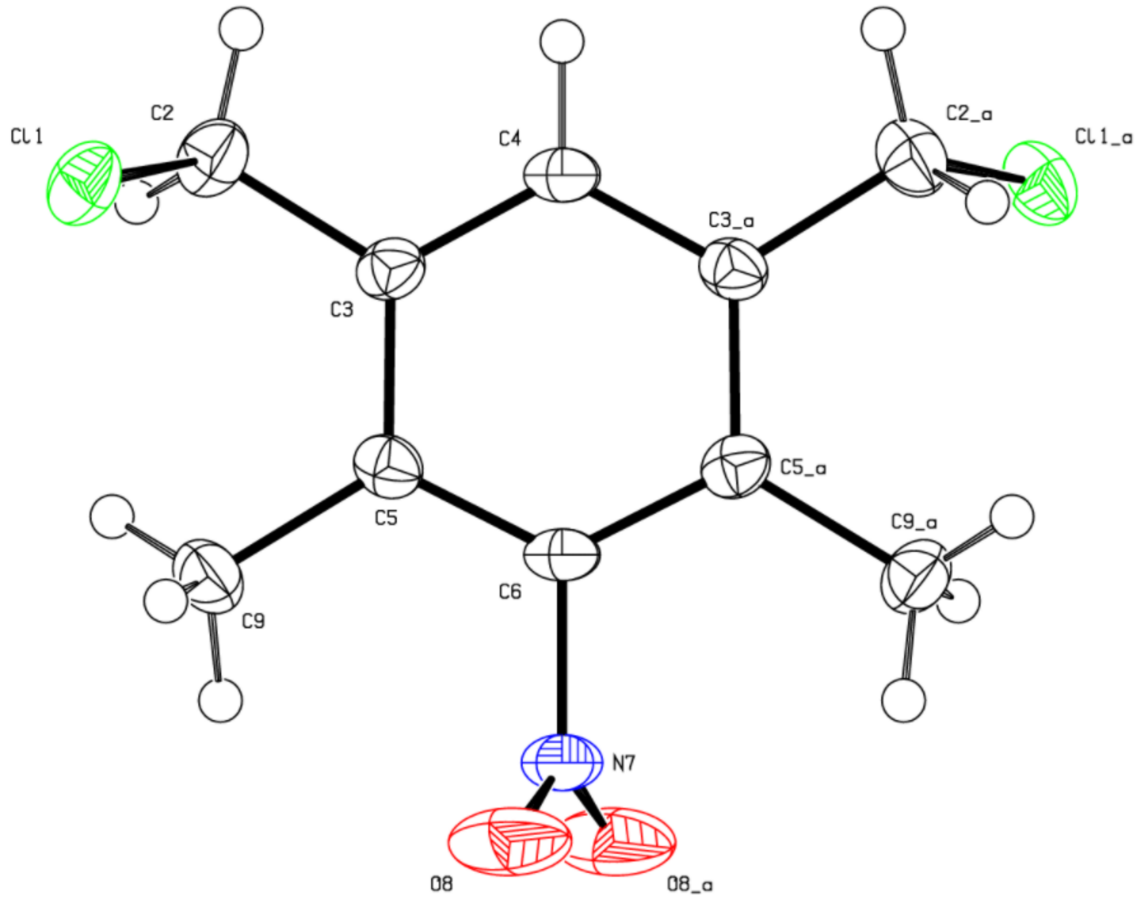

Figure S 41. Crystal structure of compound **10**, ellipsoids drawn at 50% probability.
Symmetry code: (a) 1 – *x*, *y*, 1.5 – *z*.

Table S 1. Crystallographic details for compound **10**

Formula	$C_{10}H_{11}Cl_2NO_2$
M_r	248.11
Crystal system	monoclinic
Space group	*C* 2/*c*
Z	4
a /Å	15.72720(2)
b/Å	8.273769(15)
c /Å	8.583140(18)
β / °	95.913(3)
V / Å^3	1110.923(7)
ρ_{calc} / g cm^{-3}	1.483
Crystal habit	Colourless block
Crystal dimensions /mm	0.017 × 0.031 × 0.136
Radiation	Cu K_α (1.54180 Å)
T /K	100
μ /mm^{-1}	5.101
R(*F*), *Rw*(*F*) /%	4.50, 6.89
CCDC cif deposition number	CCDC 2085509

Table S 2. Selected bond lengths (Å) and angles (°) for compound **10**

O(8) – N(7)	1.213(2)	O(8) – N(7) – O(8)[a]	124.7(3)
N(7) – C(6)	1.477(3)	O(8) – N(7) – C(6)	117.65(14)
C(2) – C(3)	1.497(3)	Cl(1) – C(2) – C(3)	110.70(16)
C(3) – C(4)	1.393(2)	C(2) – C(3) – C(4)	119.42(19)
C(3) – C(5)	1.404(3)	C(2) – C(3) – C(5)	121.17(18)
C(5) – C(6)	1.390(2)	C(4) – C(3) – C(5)	119.41(18)
C(5) – C(9)	1.507(3)	C(3) – C(4) – C(3)[a]	122.6(3)
		C(3) – C(5) – C(6)	116.12(18)
		C(3) – C(5) – C(9)	122.03(18)
		C(6) – C(5) – C(9)	121.85(19)
		N(7) – C(6) – C(5)	116.86(13)
		C(5) – C(6) – C(5)[a]	126.3(3)

Symmetry code: (a) 1 – *x*, *y*, 1.5 – *z*.

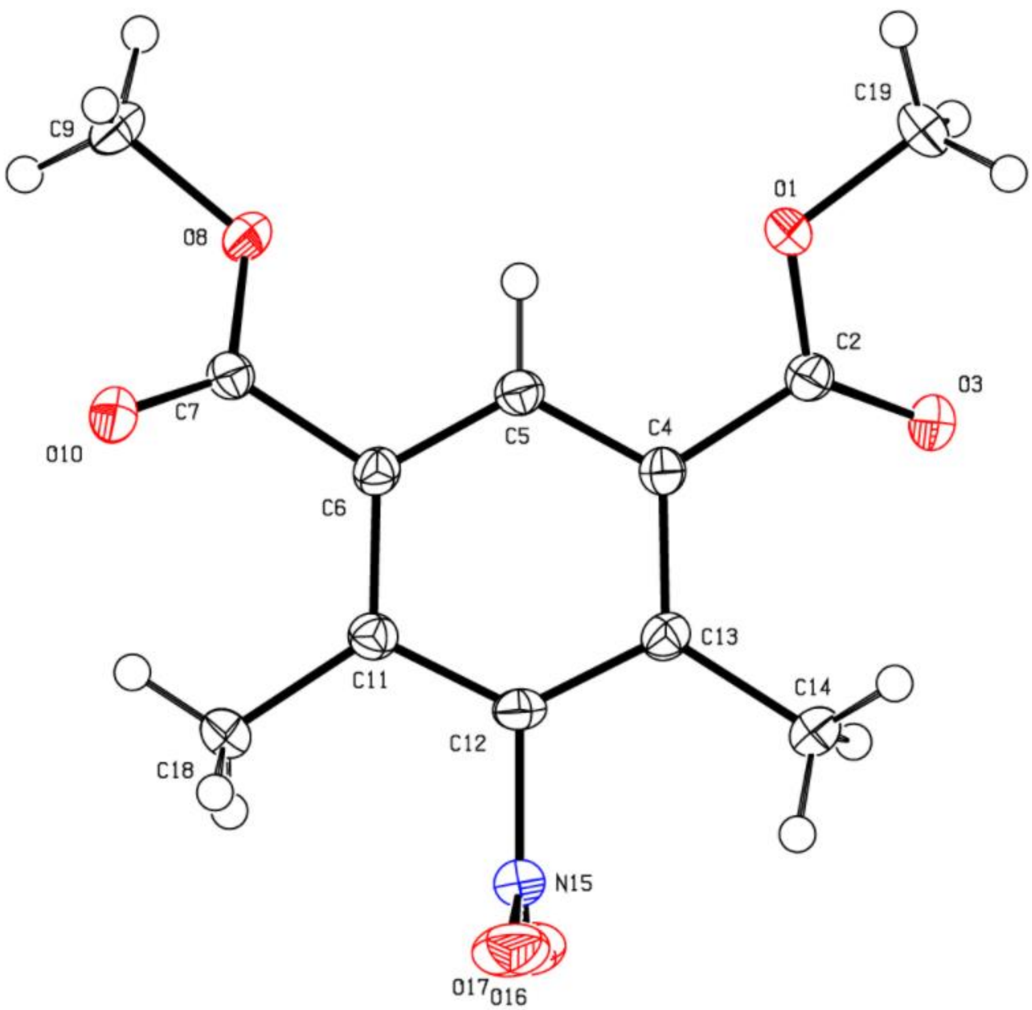

Figure S 42. Crystal structure of compound **12**, ellipsoids drawn at 50% probability.

Table S 3. Crystallographic details for compound **12**

Formula	$C_{12}\ H_{13}\ N\ O_6$
M_r	267.24
Crystal system	monoclinic
Space group	$P\ 2_1/n$
Z	4
a /Å	7.94120(1)
b/Å	17.09118(2)
c /Å	9.16055(1)
β / °	102.051(2)
V / Å^3	1215.910(11)
ρ_{calc} / g cm^{-3}	1.460
Crystal habit	Colourless block
Crystal dimensions /mm	0.030 × 0.066 × 0.098
Radiation	Cu K_α (1.54180 Å)
T /K	100
μ /mm^{-1}	1.015
$R(F)$, $Rw(F)$ /%	3.86, 5.32
CCDC cif deposition number	CCDC 2089501

Table S 4. Selected bond lengths (Å) and angles (°) for compound **12**

O(1) – C(2)	1.3375(18)	C(2) – O(1) – C(19)	114.98(11)
O(1) – C(19)	1.4461(17)	O(1) – C(2) – O(3)	123.55(13)
C(2) – O(3)	1.2121(18)	O(1) – C(2) – C(4)	111.14(12)
C(2) – C(4)	1.4912(19)	O(3) – C(2) – C(4)	125.28(13)
C(4) – C(5)	1.392(2)	C(2) – C(4) – C(5)	118.75(12)
C(4) – C(13)	1.4070(19)	C(2) – C(4) – C(13)	121.47(13)
C(5) – C(6)	1.390(2)	C(5) – C(4) – C(13)	119.77(13)
C(6) – C(7)	1.4959(19)	C(4) – C(5) – C(6)	122.56(13)
C(6) – C(11)	1.4058(19)	C(5) – C(6) – C(7)	118.11(12)
C(7) – O(8)	1.3400(18)	C(5) – C(6) – C(11)	120.03(13)
C(7) – O(10)	1.2075(18)	C(7) – C(6) – C(11)	121.83(13)
C(8) – C(9)	1.4504(18)	C(6) – C(7) – O(8)	110.58(12)
C(11) – C(12)	1.397(2)	C(6) – C(7) – O(10)	125.55(13)
C(11) – C(18)	1.5043(19)	O(8) – C(7) – O(10)	123.86(13)
C(12) – C(13)	1.393(2)	C(7) – O(8) – C(9)	116.11(12)
C(12) – N(15)	1.4783(18)	C(6) – C(11) – C(12)	115.18(13)
C(13) – C(14)	1.5109(19)	C(6) – C(11) – C(18)	124.66(13)
N(15) – O(16)	1.2215(19)	C(12) – C(11) – C(18)	120.09(13)
N(15) – O(17)	1.2214(19)	C(11) – C(12) – C(13)	127.03(13)
		C(11) – C(12) – N(15)	116.40(12)
		C(13) – C(12) – N(15)	116.57(12)
		C(4) – C(13) – C(12)	115.42(12)
		C(4) – C(13) – C(14)	123.62(13)
		C(12) – C(13) – C(14)	120.96(12)
		C(12) – N15) – O(16)	117.58(13)
		C(12) – N(15) – O(17)	117.75(13)
		O(16) – N(15) – O(17)	124.67(13)

Figure S 43. CGC determination vial inversion of gelators **2** and **3** (20 mM).

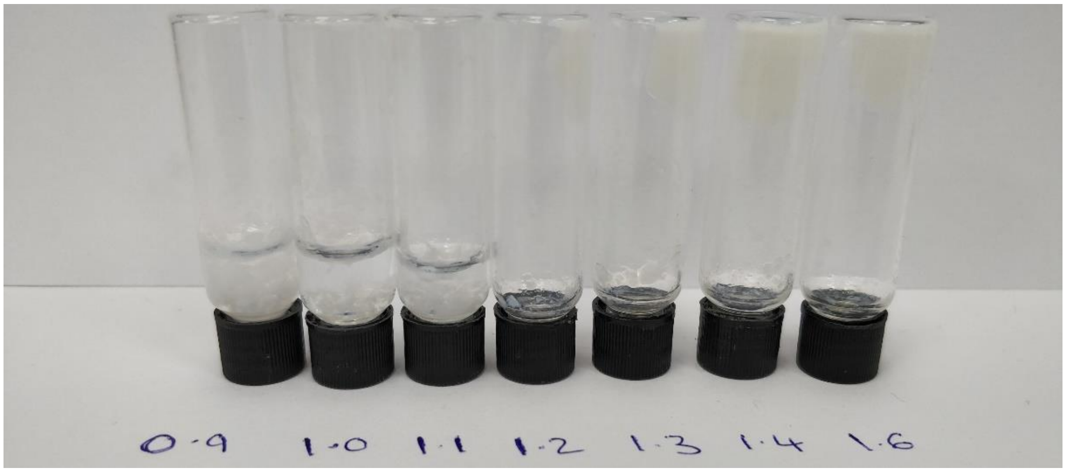

Figure S 44. CGC determination vial inversion of gelator **4**. Mass of gelator in mg written below each vial.

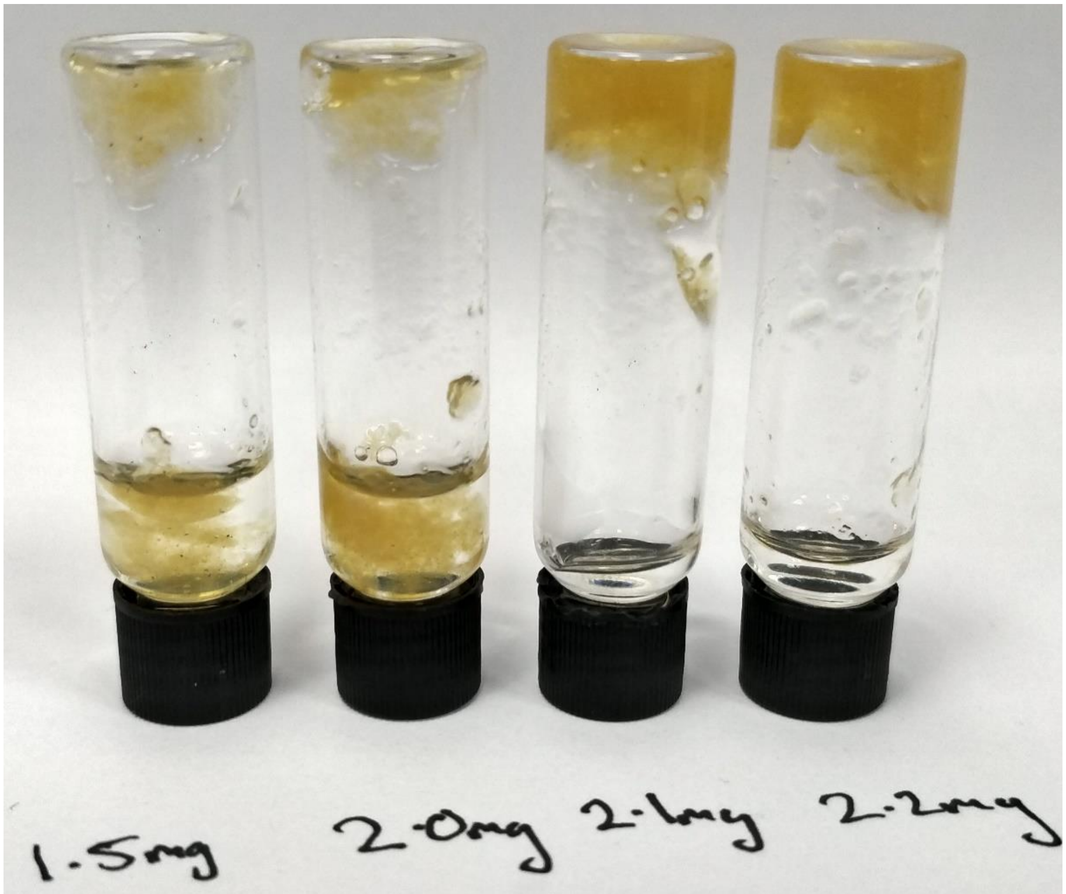

Figure S 45. CGC determination vial inversion of gelator **6**. Mass of gelator in mg written below each vial.

Figure S 46. CGC determination vial inversion of gelator **7**. Mass of gelator in mg written below each vial.

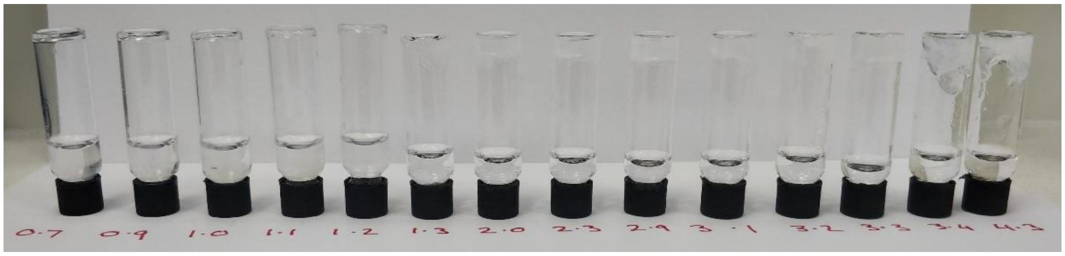

Figure S 47. CGC determination via vial inversion of gelator **8**. Mass of gelator in mg written below each vial.

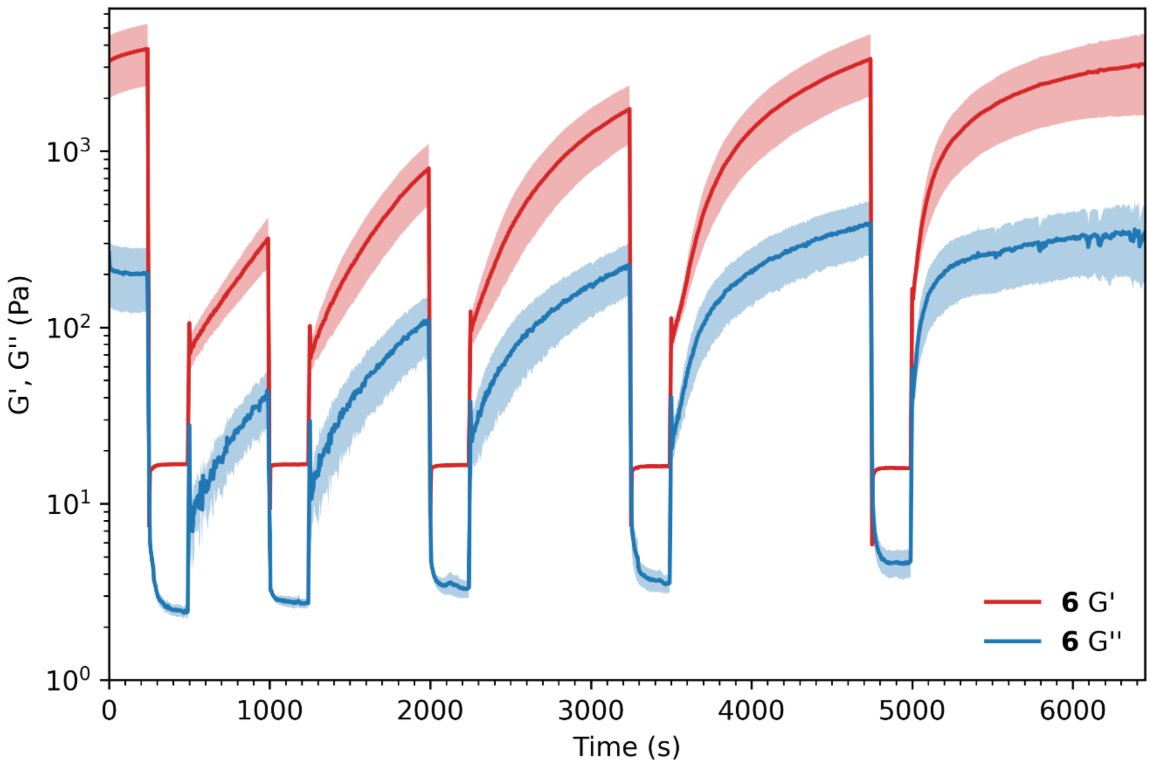

Figure S 48. Continuous step-strain measurements of **6** at 25 °C (high-amplitude oscillatory parameters: strain γ = 250%, frequency = 1 Hz, low-amplitude oscillatory parameters: strain γ = 0.1%, frequency = 1 Hz) with increasing low shear interval until complete network recovery.

Table S 5. Rheological properties of hydrogelators

	(1)	**(4)**	**(6)**	**(7)**
G'^a (Pa)	1.780E+004	2.135E+003	4.653E+003	4.935E+003
G''^a (Pa)	2.085E+003	211.9	206.8	228.5
γ_y%^b	6.77±1.48	77.14±2.60	41.02±11.15	22.56±6.88
σ_y (Pa)^c	373.40±28.17	72.65±4.87	118.35±57.60	92.21±32.69
γ_y%^c	3.71±0.70	40.61±1.63	11.36±2.96	9.85±2.17

a = observed after equilibrating for 12 hours, measured at 1Hz and 0.1% shear strain, b = determined as the % strain at the inversion of G' and G'', c = determined from peak analysis of elastic stress vs. shear strain data.

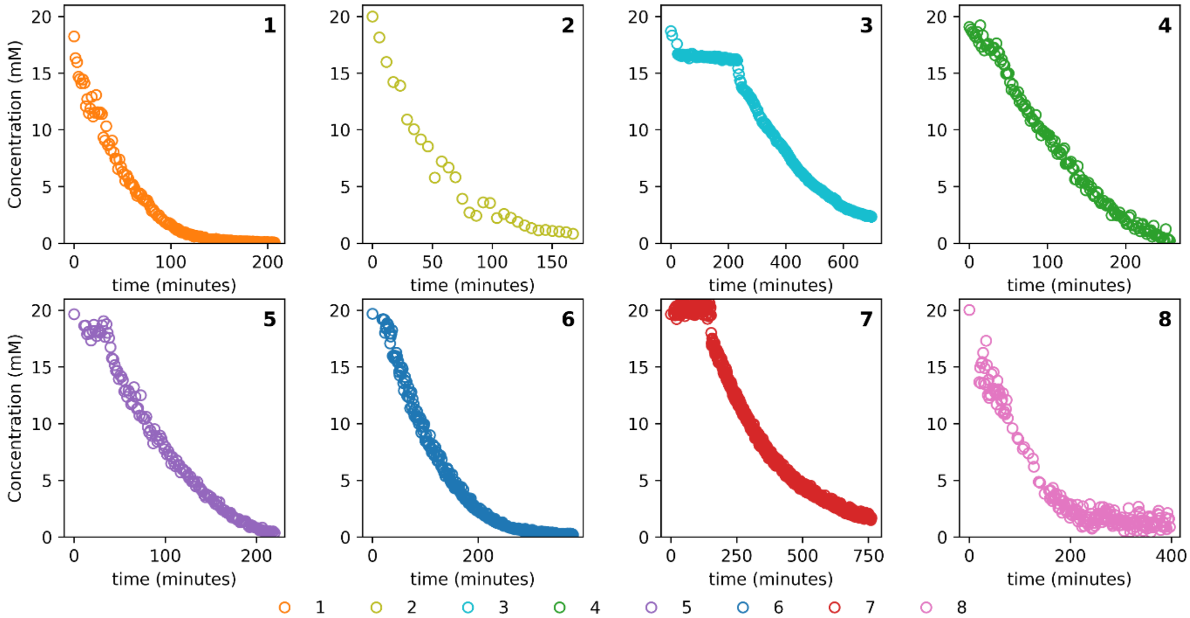

Figure S 49. Kinetics of formation of gelator networks **1** – **8** as monitored by ^{1}H NMR spectroscopy.

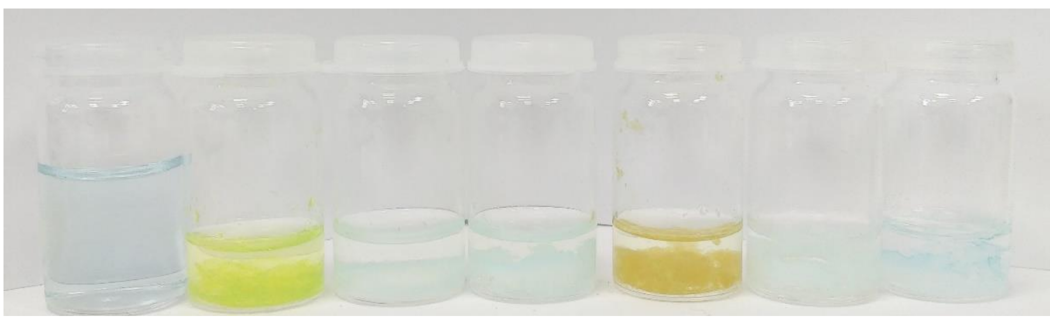

Figure S 50. From left to right: methylene blue solution (3 mL, 4 mgL^{-1}) without gelator, gelators **1**, **4**, **5**, **6**, **7**, **8** (10 mM), gelled with HCl, within 12 hours after addition of methylene blue solution (3 mL, 4 mgL^{-1}).

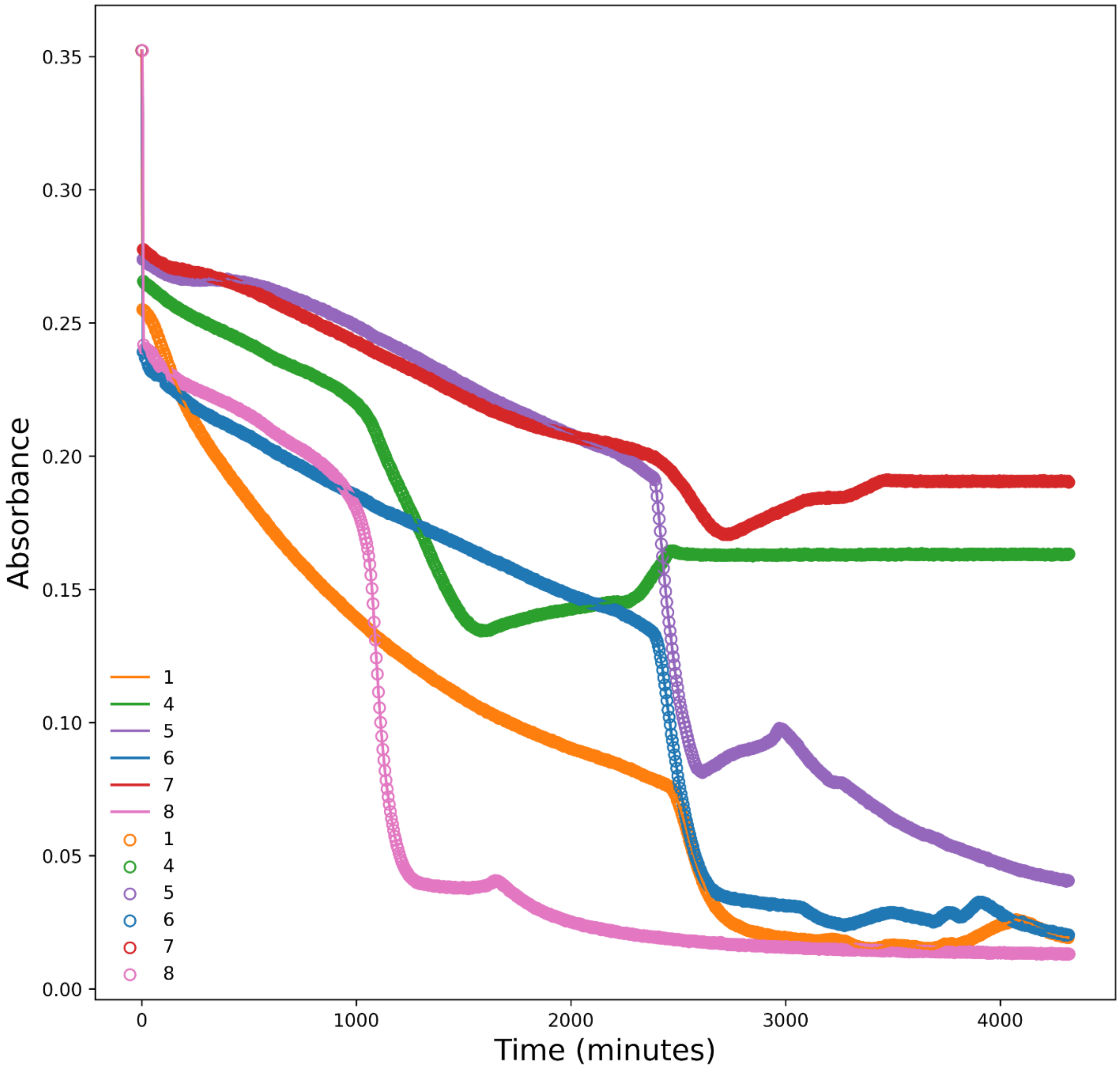

Figure S 51. Absorbance maxima of methylene blue (664 nm) *vs*. time for hydrogelators **1**, **4**, **5**, **6**, **7** and **8**.

